

Chapitre 2

Détermination du ^{231}Pa et du ^{230}Th , dans les sédiments marins, par spectrométrie de masse à source plasma et secteur magnétique: méthode, optimisation, précautions et corrections.

Introduction

The difference in particle reactivity of ^{230}Th and ^{231}Pa , combined with a constant source, have led to a number of paleoceanographic applications. Reconstruction of the past ocean circulation and productivity patterns is essential to understand the CO_2 cycle (e.g. Sigman and Boyle, 2000), in particular, and, more generally, the causes of the variability of the Earth's climate during the Quaternary. In addition, some of the proxies commonly used to reconstruct paleoproductivity like calcium carbonate (Lyle et al., 1988; Archer, 1991; Isern, 1991; Wefer et al., 1999) and barite (Paytan et al., 1996) accumulation rates, can be biased by sediment focusing or winnowing (Marcantonio et al., 2001; Pichat et al., in preparation). Therefore, the results have to be tested for sediment remobilization by using $(^{230}\text{Th})_{\text{xs},0}$ normalized flux instead of $\delta^{18}\text{O}$ -derived accumulation rate. Downcore measurements of $(^{231}\text{Pa})_{\text{xs},0}$ and $(^{230}\text{Th})_{\text{xs},0}$ in deep-sea sediments provide a means to determine the variations in the deep-water circulation or in the biological productivity, the importance sediment remobilization, and the behavior of particles in the water column.

Until now, the low precision of alpha and beta spectrometry has limited the use of ^{231}Pa and ^{230}Th as paleoceanographic proxies. In addition, the database remains patchy, especially in the ocean gyres, because of the low sample throughput of the alpha and beta spectrometry-based methods.

Here we propose a method to measure ^{231}Pa and ^{230}Th concentrations in sediments by sector field inductively-coupled plasma mass-spectrometry (SF-ICP-MS) which combines high sample throughput with high sensitivity and relatively high precision. This method has been developed in parallel for seawater samples (Choi et al., submitted) and shows promising potential for $^{231}\text{Pa}/^{235}\text{U}$ disequilibrium measurements in young volcanic rocks. A comparison of three techniques of chromatographic extraction of Th, Pa, and U is presented at the end of this chapter.

Sector Field Inductively-Coupled Plasma Mass Spectrometry Determination of ^{231}Pa and ^{230}Th in Sediments: Methodology, Optimization, Precautions, and Corrections

Sylvain Pichat¹, Ken W. W. Sims², Lary A. Ball², Roger François², Susan Brown-Leger²

¹ *Laboratoire de Sciences de la Terre, Ecole normale supérieure de Lyon, 69364 Lyon
cedex7, France*

² *Woods Hole Oceanographic Institution, Woods Hole, MA 02543, U.S.A.*

In preparation

Abstract

Usually the determination of ^{230}Th in deep-sea sediments is made by either quadrupole Inductively Coupled Plasma Mass Spectrometry (ICP-MS) or α -spectrometry, and by α -spectrometry for ^{231}Pa , resulting in errors of at least 5 % or even more than 10 % on the $(^{231}\text{Pa}/^{230}\text{Th})_{\text{xs},0}$ ratio. We have developed a method to measure both ^{230}Th and ^{231}Pa by magnetic sector ICP-MS, which greatly enhances the precision, especially for ^{231}Pa , and considerably increases the samples throughput. With this method the internal precision obtained for the $(^{231}\text{Pa}/^{230}\text{Th})_{\text{xs},0}$ ratio is typically 1.5 %. Here we discuss the relative contributions of the various corrections inherent to ICP-MS measurements of the ^{230}Th and ^{231}Pa . In the method described here, sediment samples (*ca.* 200 mg) were spiked with ^{229}Th and ^{233}Pa before dissolution and pre-concentration using a conventional method of Fe-hydroxide co-precipitation, followed by anion-exchange chromatographic separation. One aliquot was previously set aside to jointly measure - by isotopic dilution with ^{229}Th and ^{236}U spikes - the ^{232}Th and ^{238}U concentrations, employed to evaluate the terrigenous and authigenic contributions

corrections. Measurements were performed with a Finnigan MAT Element magnetic sector ICP-MS, in low resolution mode. Samples were injected with a Membrane desolvator equipped with a PFA microconcentric nebulizer. The internal precision of the measurement was $> 0.5\%$ (2σ level) for all isotopes. The signals were corrected with a specially written Matlab[®] program from the contributions of the background noise, ^{232}Th tailing, hydrides isobaric interferences, instrumental mass bias, procedural blank, detrital and authigenic fractions of the sediment. The overall reproducibility on the basis of replicate measurements of the $(^{231}\text{Pa}/^{230}\text{Th})_{\text{xs},0}$ ratio was estimated to be 4.5% (2σ level). This method has been successfully applied to downcore profiles in the equatorial Pacific, which show a remarkable internal consistency.

1 - Introduction

Determination of ^{231}Pa and ^{230}Th in oceanic sediments appears as important to understand boundary scavenging processes (Nozaki et al., 1981; 1985 Bacon and Anderson, 1983; Anderson et al., 1983a,b; Bacon, 1984;1988; Huh and Beasley, 1987; Cochran, 1992; Luo et al., 1995; Stephens and Kadko, 1997; Edmonds et al., 1998), sediment redistribution by deep currents (Suman and Bacon, 1989; François et al., 1990; 1993; Frank et al., 1999; Marcantonio et al., 2001; Pichat et al., in preparation), and hydrothermal activity (Kadko, 1980; Shimmiel and Price, 1988; Frank et al., 1994). The $(^{231}\text{Pa}/^{230}\text{Th})_{\text{xs},0}$ ratio (the subscript xs denotes the activity in excess and the subscript zero denotes the decay correction to the time of deposition) in deep-sea sediments has been used to reconstruct deep-water circulation in the Atlantic and the Southern Ocean (Bacon and Rosholt, 1982; Mangini and Kühnel, 1987; Moran et al., 1997; Yu et al., 1996; 1994; François et al., 2000), as well as paleoproductivity variations (Lao et al., 1992; Kumar et al., 1993; 1995; François et al., 1997; Walter et al., 1997; 1999; Pichat et al., in preparation) over the last 200,000 years. However, the lack of a method which combine precision with a high sample throughput has limited, until now, the application of ^{231}Pa and ^{230}Th as paleoceanographic proxies. For example, the lack of precision in the measurements did not allow one to distinguish variations in $(^{231}\text{Pa}/^{230}\text{Th})_{\text{xs},0}$ ratio in sediments located in the north Pacific gyre. Precise measurements would give

information on the dominant process that scavenged Pa during the last glacial maximum. In addition, the $(^{231}\text{Pa}/^{230}\text{Th})_{\text{xs},0}$ database in the Atlantic does not allow a determination of the strength of the thermohaline circulation during the last glacial period within the 20 % accuracy expected from model calculations (Marchal et al., 2000). Both an extension of the dataset and more precise measurements are needed to solve these problems.

Until the end of the 90's, ^{231}Pa and ^{230}Th measurements in sediment samples were made by α -spectrometry (e.g. Anderson et al., 1983a; Lao et al., 1992; François et al., 1993; Kumar et al., 1993; 1995). The precision was typically of 5 to 10 %. ^{230}Th has also been measured by single collector Inductively Coupled Plasma Mass Spectrometry (ICP-MS) using isotope dilution technique with a ^{229}Th spike (e.g. Shaw and François, 1991; Yu et al., 1996, Marcantonio et al., 2001). However, ^{231}Pa was still measured by α -spectrometry, which accounts for most of the imprecision in the $(^{231}\text{Pa}/^{230}\text{Th})_{\text{xs},0}$ ratio measurements. ^{231}Pa is a α -emitter and the yield monitor, ^{233}Pa , is a β -emitter. This situation prevents direct counting of $^{231}\text{Pa}/^{233}\text{Pa}$ ratios and requires an accurate evaluation of the efficiency of the α and β counters. ^{231}Pa has also been measured by counting its β -emitter daughter, ^{227}Th , thus avoiding the chemical separation of protactinium (Bernat and Goldberg, 1969; Mangini and Sonntag, 1977; Kadko, 1980; Stephens and Kadko, 1997). However, the β peaks of ^{227}Th (5.908 and 6.037 MeV) overlap with the peaks of ^{212}Bi (6.04 and 6.08 MeV), thus implying corrections to remove the ^{212}Bi contribution. Also, ^{227}Th requires large amounts of samples (typically *ca.* 3 g of sediment) and counting times of the order of 100 hours to attain a precision of only 5 - 10 %. In addition, this precision rapidly decreases downcore because of the ^{231}Pa decay (table 1). In spite of the wide utilization of Thermal Ionization Mass Spectrometry (TIMS) for the measurement of U-Th and U-Pa disequilibria in young volcanic rocks (Goldstein et al., 1993; Pickett and Murell, 1997; Bourdon et al., 1998; Sims et al., 1999; in press), corals (Edwards et al., 1997), and more recently, for the measurement of ^{231}Pa and ^{230}Th in ocean waters (Edmonds et al., 1998), to date no measurements by this technique for deep-sea sediments have been reported for $(^{230}\text{Th}/^{231}\text{Pa})_{\text{xs},0}$ or ^{231}Pa , and only a few reports have dealt with ^{230}Th (Henderson and Slowey, 2000). While high precision is achieved by TIMS, the ionization potential of Th and the long time required for sample analysis limit the application. Another disadvantage of ^{231}Pa TIMS analyses arises from

the need to perform the measurement immediately after sample preparation (Pickett et al., 1994; Edmonds et al., 1998; Bourdon et al., 1999) because of the short half-life of the ^{233}Pa spike ($t_{1/2} = 26.967$ days) (Firestone, 1996) and because U and Pa are not ionized at the same temperature in TIMS.

Here we report a method for the measurement of ^{231}Pa and ^{230}Th by sector type ICP-MS. The method requires small amounts of deep-sea sediments (typically *ca.* 100-300 mg). The high sample throughput, high sensitivity (*ca.* 5.10^6 counts / ppb) and relatively high precision (*ca.* $< 0.5\%$ (2σ level)) for ^{231}Pa and ^{230}Th concentrations represent significant improvements over the alpha α -spectrometry methods. Compared to TIMS, this method represents a significant improvement since it allows the measurement of more than 20 samples per day with a precision close to those attainable by TIMS. Additionally, sector field ICP-MS (SF-ICP-MS) offer the advantage of having a very low background noise, hence contributing to lower the detection limits to the low fg/g level (Kim et al., 1991; Field and Sherrell, 1998; Rodushkin et al., 1999). However, several variables during the sample processing (yields, blanks) and the ICP-MS analysis (blanks, dark noise, isobaric interferences, instrumental mass bias, tail corrections) can significantly influence the reliability, accuracy and precision of the results obtained. The question of these influences is addressed in this report.

While this procedure is described with an emphasis upon the analysis of ^{230}Th and ^{231}Pa in sediment samples, it is clearly applicable to volcanic rocks, as is illustrated by the fact that our spike calibration procedure involves the measurement of ^{231}Pa in both young and old volcanic rocks.

2 - Experimental

2.1 - Materials

2.1.1 - Sample materials

Samples originating from the equatorial Pacific and containing 60-90 wt.% CaCO_3 were examined to determine the precision of the method and several replica were carried out to test the validity and further assess the precision of the method. These samples were collected in the western Pacific warm pool (core MD97-2138) and the eastern equatorial Pacific (core ODP leg 138 site 849). The results are reported and discussed elsewhere (Pichat et al., in preparation). Only the analytical aspects are discussed hereafter.

2.1.2 - Purities of the inorganic acids used and cleaning of the containers

HCl, HNO_3 and HF reagent grade acids pro analysis were used for dissolution and cleaning procedures. High purity acids (SeastarTM) were employed to introduce the sample into the ICP-MS. All Teflonware, HDPE containers and resins were thoroughly acid cleaned; in particular, the Teflonware was cleaned with 9 N HCl - 0.13 N HF to remove any contamination by Pa. The very low blanks level recorded showed that the use of reagent grade acids is appropriate for the measurement of ^{231}Pa and ^{230}Th in sediment samples (see section 5.1). This is also due to the high ^{231}Pa and ^{230}Th content of the sediments. An additional reason for choosing reagent grade acids is their low cost. However, the use of high purity acids is required for seawater samples (Choi et al., submitted) and to obtain higher precision. We also suggest the use of high purity acids to apply the technique presented hereafter to young volcanic rocks. High purity acids were used for spike calibration because they provide a lower uncertainty because of lower blanks.

2.2 - Sample preparation

The sediment samples were first dried in an oven at 333-343 K for 3 days. They were then crushed in an agate mortar which has been previously cleaned with successive treatments of acid washed silica, ethanol, and Milli-Q water, and then pre-contaminated with a small portion of the sample, in order to avoid sample cross-contamination. The resulting powder was then thoroughly homogenized.

Carbonates were eliminated as CO_2 by adding 2-4 ml of 2 N HCl to 150-300 mg of the sediment powder. To limit sample splatter due to CO_2 degassing, 1-2 ml of Milli-Q water were added before the HCl and lids were put on the Teflon[®] TFE beakers to avoid losing material. After carbonate removal, ^{233}Pa (0.5-1 pg) and ^{229}Th (*ca.* 100 pg) spikes were added to the suspension before dissolution in a mixture of 15 ml of 8 N HNO_3 , 5 ml of concentrated HF and 7 ml of concentrated HClO_4 . The solution was left overnight to achieve sample dissolution and spike-sample equilibration. It was then evaporated to semi-solid at 473 K. During this step of the procedure, the beakers were covered with teflon “watch glass” so that the perchloric acid was constantly refluxed as it dried. This refluxing is critical for mineralizing organic matter, spike-sample equilibration, and to destroy fluoride complexes which can negatively influence the yields during separation and purification steps. In the course of the evaporation, 2-3 ml of concentrated HF was added, and 8 N HNO_3 was used several times to wash beaker walls. After complete dissolution and evaporation to near dryness, 20 ml of 2 N HCl was added to the semi-solid sample so that it was completely in solution. The resulting solution is then split into two aliquots. One aliquot, hereafter referred to as the ^{231}Pa - ^{230}Th aliquot, was used for ^{231}Pa and ^{230}Th analyses. The other aliquot, hereafter referred to as the ^{238}U - ^{232}Th aliquot, and corresponding to approximately 2 mg of sediment, was used for ^{238}U and ^{232}Th measurements.

2.2.1 - ^{231}Pa and ^{230}Th separation

The pH of the ^{231}Pa - ^{230}Th aliquot was increased to 8-9 by adding ~10 ml of concentrated NH_4OH to precipitate iron oxyhydroxides. Because Pa and Th have a high affinity for iron oxyhydroxides they are quantitatively entrained in the precipitate.

Additionally, fluoride ions remained into the solution, thus avoiding the further formation of stable fluoride complexes (PaF_7^{2-}) (Guillaumont et al., 1968) which would compromise the efficiency of the following protactinium elution. The precipitate was cleaned by successive dissolutions and reprecipitations. It was first dissolved by adding 5-10 ml of Milli-Q water and reprecipitated by addition of a few drops of concentrated NH_4OH . This operation was repeated using 2-8 ml of 2 N HCl instead of H_2O . Finally the precipitate was dissolved by adding a volume of 12 N HCl equivalent to three times the volume of iron oxyhydroxide. This step is important as both an initial purification step and as a means of removing F ions.

Th and Pa were separated by anion exchange. The procedure was modified from the method described by Anderson and Fleer (1982) and Fleer and Bacon (1991). A 4 ml column of AG1-X8 resin (100-200 mesh) packed into a 0.6 x 20 cm polyethylene tube ended by a polyethylene frit (KONTES™) was pre-conditioned with 16 ml of 9 N HCl. The dissolved sample, usually 9-15 ml, was passed through this column which was subsequently rinsed with 12 ml of 9 N HCl. In chloride form, Th passes through the column and was recovered in the wash/filtrate. Pa on the other hand was adsorbed on the column together with Fe and U and was subsequently eluted with 12 ml of 9N HCl - 0.13 N HF and collected into a PTFE Teflon® beaker. Most of U and Fe remain on the column which was discarded.

To further purify the Th, this fraction was run through an additional HNO_3 anion column. The Th fraction from the previous column was evaporated to near dryness, taken up into 8 ml of concentrated HNO_3 and then evaporated to 1 ml to convert it to its nitric form. One ml of Milli-Q water and 10 ml of 8N HNO_3 were then added to the Th fraction and the resulting solution was then loaded on a 4 ml AG1-X8 column, washed with HCl and pre-conditioned with 16 ml of 8N HNO_3 . The column containing the Th was rinsed with 16 ml of 8N HNO_3 and the Th was eluted with 12 ml of 9N HCl and collected in a PTFE Teflon® beaker.

To separate U and Pa and further purify the Pa, the Pa fraction (12 ml) is spiked with ^{236}U (75 pg) and equilibrated overnight at 323-333 K with the lid closed; this ^{236}U spike is used to monitor the Pa-U separation. This Pa fraction, in 9N HCl – 0.13 N HF, is

then passed through another 4 ml AG1-X8 column pre-conditioned with 16 ml of 9 N HCl to achieve an optimal separation between Pa and U. The column was further eluted with 12 ml of 9N HCl - 0.13N HF and the total eluate was recovered in a PTFE Teflon[®] beaker. U was eluted successively with 2 ml of Milli-Q water and 10 ml of 1 N HBr. The eluate was recovered in a PTFE Teflon[®] beaker.

The Th and Pa solutions were each evaporated to a drop. 0.5 ml of 8 N HNO₃ or 8 N HNO₃ - 0.05 N HF were added to the Th or Pa fractions, respectively which were again evaporated to a drop to achieve the conversion to nitric form. The addition of low concentrated HF allows the storage of the Pa solution because fluoride ions stabilize Pa as PaF₇²⁻ anions thereby preventing the formation of hydroxocomplexes and their polymerization (Guillaumont et al., 1968). Before analysis, 350 µl of 0.05 N HF was added to the Pa fraction and the closed vial heated to 333 K in a drying oven overnight in order to prevent the loss of Pa via hydroxocomplexes on the walls of the vial. 0.3-0.5 ml (depending on the nebulizer uptake rate) of Milli-Q water was added to the Th fraction. U samples were evaporated to dryness before adding 0.3-0.5 ml of 0.8 N HNO₃.

The resulting solutions were finally filtered through acid-washed Acrodisk[™] filters (0.2 µm pore size) to prevent clogging of the micronebulizer by particles that could have remained in the solution.

Recoveries of ^{233}Pa from the anion-exchange columns were 98 % (± 8 %) as estimated from γ -counting experiments made at the ENS Lyon. It is in good agreement with the results found with tracer experiments by Choi et al. (submitted).

2.2.2 - ^{238}U and ^{232}Th spiking

^{238}U and ^{232}Th measurements are required to correct the ^{231}Pa and ^{230}Th concentrations in the sediment resulting from the contribution of the detrital and the authigenic fractions. The detrital fraction comes essentially from continental erosion and is transported to the ocean mainly by eolian, ice and riverine inputs. The authigenic fraction comes from the *in situ* ingrowth of ^{231}Pa and ^{230}Th resulting from the decay of ^{235}U , ^{234}U , and ^{238}U in the sediment.

The ^{238}U - ^{232}Th aliquot was spiked with ^{236}U (*ca.* 7 ng) and ^{229}Th (*ca.* 2.3 ng) and then diluted by 10 ml of Milli-Q. The solution was left several days to achieve spike-sample equilibration before analysis by SF-ICP-MS. The contribution of the spiking of the whole sample by ^{229}Th prior to dissolution (section 2.2) represents less than 0.3 ‰ of the total ^{229}Th signal. It was therefore neglected in the isotopic dilution calculations.

2.3 - Analysis by SF-ICP-MS

2.3.1 - Measurements of isotopes concentrations

^{230}Th and ^{231}Pa concentrations are determined by isotope dilution as calculated from the $^{230}\text{Th}/^{229}\text{Th}$ and $^{231}\text{Pa}/^{233}\text{Pa}$ (Pa; U) ratios measured with a magnetic sector ICP-MS (Finnigan MAT Element I) in low-resolution mode (mass resolving power $\Delta m/m = 300$). The standard operating parameters used during these analyses are given in table 2. Samples were introduced into the plasma through a membrane desolvator (MCN-6000, Cetac Technologies) equipped with a PFA microconcentric nebulizer and a redesigned PFA spray chamber (Elemental Scientific Inc.) heated at 373 K. The redesigned chamber improved plasma stability by more efficiently removing wet droplets which could have passed through the plasma (Niu and Houk, 1996). Passive aspiration was used to improve the stability of the ion beam and eliminate possible memory effects which might have stemmed from the PVC tubes of a peristaltic pump. Combining the MCN-6000 and PFA microconcentric nebulizer significantly reduces the sample uptake rate to 80-150 $\mu\text{l}/\text{min}$ and improves sensitivity to 4-8 10^6 cps/ppb U, i.e. by a factor of 5 to 10 with respect to standard pneumatic nebulization, without increasing background counts. This results in an overall efficiency (ions detected / atoms introduced) similar to TIMS, that is *ca.* 1 ‰. Measurements were made in the electrostatic scanning mode (i.e. by changing the acceleration voltage) over a range of masses that are indicated for each isotope in table 3. The width of each scanned peak was adjusted to record the flat top area and thus maximize the precision of the data. Data acquisition time was 2-3 minutes for each fraction.

Between each sample, or every two samples for the ^{238}U - ^{232}Th aliquot, the $^{235}\text{U}/^{238}\text{U}$ ratio of a standard uranium solution (NBS 960, $[^{235}\text{U}/^{238}\text{U}] = 137.88$) was determined to correct for mass bias fractionation (see section 3.6).

Great care was taken to eliminate carry over, or cross contamination by the samples by washing with high purity (Seastar™) 0.8 N HNO_3 , after each U and Th analysis, and a 0.8 N HNO_3 - 0.05 N HF mix after Pa analysis, sample until the signal intensities had returned to background levels. In addition to this extensive washing, before each measurement, including that of NBS 960, blanks were determined to correct for residual carry over between samples and instrumental background noise.

2.3.2 - Decay of ^{233}Pa in ^{233}U : implications for ^{231}Pa measurements and ^{233}Pa spike calibration

An optimal separation between Pa and U is required because ^{233}U , produced by decay of ^{233}Pa , is undistinguishable from ^{233}Pa by ICP-MS as both are efficiently ionized with a plasma source. Since ^{231}Pa is quantified from the $^{231}\text{Pa}/^{233}\text{Pa}$ ratio measured in the Pa eluate, any ^{233}U bleeding from the column would increase the ^{233}Pa signal intensity and thus affect the $^{231}\text{Pa}/^{233}\text{Pa}$ ratio. Adding ^{236}U prior to the last Pa column enables one to quantify the possible U contribution to the signal at mass 233. The contribution was calculated by comparing the measurements of the ratios between the 233 and the 236 mass peaks in the final Pa fraction and the $^{233}\text{U}/^{236}\text{U}$ in the U fraction eluted from the last Pa column. The separation of U and Pa was very efficient, only 0.05 to 0.8 % of the added ^{236}U passed through the column. Although the correction was usually negligible, the ^{233}U bleeding in the Pa fraction was, nevertheless, systematically monitored for each sample since this can be done very quickly and provides an efficient means of controlling the quality of the Pa measurements.

With ICPMS, it is not necessary to measure the $^{231}\text{Pa}/^{233}\text{Pa}$ ratio immediately after the U-Pa separation, as U and Pa are ionized with the same efficiency. Therefore, the number of counts measured on mass 233 (n_{233}) is given by (1):

$$n_{233} = n_{233\text{Pa,m}} + n_{233\text{U,m}} \quad (1),$$

where $n_{233\text{Pa},m}$ and $n_{233\text{U},m}$ are the number of atoms of ^{233}Pa and ^{233}U , respectively, at the time of measurement. Since the separation between Pa and U in the last column is greater than 99 %, and systematically checked for each sample, we assume that each atom of ^{233}U produced after the separation will come from the decay of one atom of ^{233}Pa . Because Pa and U are ionized equally in the plasma, and the number of atoms of 233 is conserved, the total 233 signal measured represents the ^{233}Pa concentration in the sample after separation. We therefore decay correct the spike to the date of separation rather than the date of analysis. This is unlike TIMS, where the spike is decay corrected to the date and time of analysis, which must be completed immediately after the final U-Pa separation column. This is because with TIMS, Pa and U ionize at different temperatures and therefore getting an accurate value for the measured 231/233 ratio requires to have “burned off” the U prior Pa to analysis.

2.4 - Spike Calibrations

2.4.1 - ^{229}Th , ^{233}U and ^{236}U spike calibration

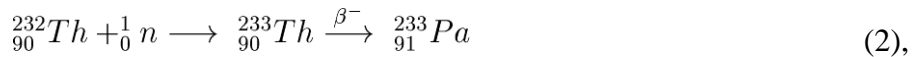
The ^{229}Th spike was used at two concentrations to quantify ^{230}Th and ^{232}Th . The ^{229}Th spike was calibrated by isotopic dilution (ID) SF-ICP-MS against a ^{232}Th gravimetric standard. The ^{236}U and the ^{233}U spikes were both calibrated by ID-SF-ICP-MS against a ^{238}U gravimetric standard. Additionally, the calibration of the two spikes was checked by cross-calibration. Typical precisions on these spike calibrations are indicated in table 4.

The ^{229}Th , ^{236}U and ^{233}U spikes calibrations were checked using the secular equilibrium between ^{230}Th and ^{238}U . ^{232}Th and ^{238}U concentrations in the 29 Ma Table Mountain Latite (TML) were measured by ID-SF-ICP-MS with the ^{229}Th spike and the ^{236}U or the ^{233}U spikes alternatively. The $^{232}\text{Th}/^{230}\text{Th}$ ratio in the TML was determined by Secondary Ion Mass Spectrometry (SIMS) (Layne and Sims, 2000, Sims et al., in press). The ($^{230}\text{Th}/^{238}\text{U}$) activity ratio was calculated from these measurements and was found to be less than 3 % off the secular equilibrium.

The validity of the ^{229}Th and ^{236}U spikes was further checked by measuring the ^{232}Th and ^{238}U concentrations in an AThO solution. AThO is a homogenous rock which has been previously measured for ^{232}Th and ^{238}U concentrations by TIMS.

2.4.2 - ^{233}Pa Spike Calibration

The ^{233}Pa spike was produced by neutron activation of ^{232}Th (2).



^{233}Th decays rapidly to ^{233}Pa ($t_{1/2}=22.3$ min) (Albert, 1982). ^{233}Pa was purified by anion AG1-X8 resin according to the procedure of Anderson and Fleer (1982). The ^{233}Pa solution was calibrated by ID-SF-ICP-MS with the ^{231}Pa of a Table Mountain Latite (TML) solution. TML is a widely used rock standard in which ^{235}U and ^{231}Pa , as well as ^{238}U and ^{230}Th , are known to be in secular equilibrium. However, the rock is not homogenous. The ^{231}Pa concentration in the TML was calculated on the basis of the ^{235}U - ^{231}Pa secular equilibrium, using the ^{235}U concentration determined by ID-SF-ICP-MS against a ^{236}U spike. Typical precision on this spike calibration is indicated in table 4.

In addition we have taken advantage of the rapid decay of ^{233}Pa in ^{233}U and the fact that Pa and U are ionized equally with ICP-MS to check the calibration of the ^{233}Pa spike. After it decayed for more than six half-lives, $n_{233\text{Pa},m}$ is close to 0, therefore, (1) become (3):

$$n_{233} = n_{233\text{U},m} = n_{233\text{Pa},0} \quad (3),$$

and provides the concentration of the ^{233}Pa spike solution. We determined the ^{233}U concentration by ID-SF-ICP-MS against a ^{238}U gravimetric standard and against a ^{236}U spike to confirm the ^{233}Pa calibration made against the TML rock standard.

Finally, the accuracy of the ^{233}Pa spike concentration was checked by ID-SF-ICP-MS against a ^{231}Pa standard which has been calibrated by ID-SF-ICP-MS against a previous ^{233}Pa spike.

The cross-calibrations between spike and standards, standards and rocks (TML and AThO), and spikes and rocks, performed by different users with different types of

instruments provide a unique means of detecting errors and achieving high precision in the spike calibrations used in the studies based on uranium-decay series.

3 - Mass Spectrometry

Corrections are needed to account for instrumental background noise, ^{232}Th interferences due to peak tailing, isobaric interferences linked to hydride formation, dark noise, instrumental mass fractionation, contamination linked to the chemical procedure and with samples spiking. These corrections and their relative influences on the measured concentrations are discussed in the following sections.

3.1 - Choice of the peak width used to measure ^{231}Pa and ^{230}Th concentrations

Sector type ICP-MS improves the accuracy compared to quadrupole ICP-MS because it produces peaks with flatter tops (figure 1). Two analytical techniques have been tested. Initially, wide peaks were measured (figure 2a,c) and the flat part of the peak showing the highest values was later extracted using an Excel spreadsheet (figure 1). Scanning wide peaks, particularly when they are flat-topped, has the disadvantage of increasing the time spent to scan each mass and thus reduces the number of ratios collected. In addition, wide peaks and slow scan times increase the risk of undergoing signal variations associated with instabilities in the plasma, the argon flow rate, the sample uptake rate, and the detector response, as well as with electronic noise (Gwiazda et al., 1998). To mitigate these effects the measured peak widths were reduced (table 3, figure 2b,d). The difference between $(^{231}\text{Pa}/^{230}\text{Th})_{\text{xs},0}$ values measured for two replica, by the two methods, was within the internal precision of both methods. The reduction of the measured peak width slightly improved the internal precision of the analysis, e.g. for ^{231}Pa the average precision was *ca.* 0.35 % instead of *ca.* 0.5 % (2σ level) with wider peaks. Additionally, data with very low precision were not found ($> 2\%$ at 2σ level) when using narrower peaks. Moreover, since the peak width for each mass is not is not

chosen by the experimentalist off line, data processing can be automated saving considerable time, post analysis.

3.2 - Background noise

The background noise is generated by the combination of the memory effect of the injection device (tubing, nebulizer, spray chamber, torch, and skimmer cones), the contribution of the inorganic acids used to inject the sample into the ICP-MS, and the dark noise of the instrument.

Input of the short-lived β -emitter ^{233}Pa on the first dynode of the ion-counting device can also increase dark noise. After the analysis of more than three hundreds ^{231}Pa samples (sediment and seawater) over one year, the dark noise of the WHOI instrument is comparable (0.2 ± 0.05 cps) to its original value (typically < 0.3 cps). Choi et al. (2001) have also recorded an increase of the dark noise, from 1.1 ± 0.1 to 1.4 ± 0.1 (95 % CI), after analysis of thirteen sediment samples. However, with ICP-MS, the dark noise is insignificant relative to the other contributions and is taken into account in the total background noise correction. Before each sample analysis, the background was determined by injecting an acid solution similar to the one used to introduce the sample. For U and Pa, the background noise was usually less than 1 % of the signal (typical values are reported in table 5). However, higher backgrounds were recorded for the thorium measurements due to the memory effects in the sampling tube and the ICP source (nebulizer through extraction lenses) (table 5). In particular, the background for the ^{232}Th concentration measurement in the sediment samples typically accounted for more than 2 % of the signal, and therefore was corrected. Also, the ^{238}U background tended to increase with the number of successive measurements (figure 3). Dark noise could not be involved to account for this progressive background increase during one series of measurements as a similar phenomenon occurred independently from the injection of short live isotopes in the system. This phenomenon reflected the progressive contamination of the injection system by the samples. Even though the background is generally negligible compared to the signal intensity of the sample, the background (using the same concentration of acid used for sample introduction) was measured before

and after each analysis. These bracketing values are then averaged and subtracted from the samples signal intensity.

3.3 - Abundance sensitivity: Correcting for ^{232}Th peak tailing

The abundance sensitivity ($\Delta m/m$) of the Finnigan MAT Element is approximately 5 ppm at 1 a.m.u.. Assuming a 99.5 % separation between Pa and Th, the concentration of both isotopes in the analyzed samples (^{232}Th ca. 3.7×10^{15} atoms/g in MD2138, 6.5×10^{15} atoms/g in ODP 849; ^{231}Pa ca. $> 10^{10}$ atoms/g in MD 2138, $> 2 \times 10^{10}$ atoms/g in ODP 849) allowed us to calculate a $^{232}\text{Th}/^{231}\text{Pa}$ ratio of 1700 and 160 in the MD 2138 and ODP 849 sediments, respectively. Because the abundance of ^{232}Th is considerably larger than that of adjacent isotopes of interest (229, 230, 231, 233), the signals must be corrected for ^{232}Th tailing (figures 2 and 4).

The ^{230}Th and the ^{229}Th signals were thus corrected using the 229.5 and 230.5 masses. In addition, the shape of the tailing was evaluated by recording mass 231.5 in order to check the validity of the correction. ^{232}Th tailing represents 500-1500 cps for ^{230}Th ($\sim 125,000$ cps) and was found to be usually negligible (50-200 cps) for ^{229}Th (500,000 cps) (figure 4a).

The ^{231}Pa signal was similarly corrected by use of the masses 230.5 and 231.5. The ^{232}Th tailing represents a contribution of 0-20 cps, i.e. < 0.5 % of the mass 231 signal (4250 cps) (figure 4b). This contribution was greatly minimized by the efficient chromatographic separation of the two elements. The difference in this contribution between sediment (< 0.5 %) and seawater (< 5 %) (Choi et al., 2001) comes from the higher number of counts in the sediment: ~ 4250 cps compared to ~ 700 cps, as well as from the low detrital content of the sediments analyzed in this study (Pichat et al., in preparation). ^{232}Th tailing interferences are expected to be greater in sediment samples from the Atlantic Ocean and, more generally, from regions submitted to intense detrital discharges.

The peak width reduction led to a better correction of the ^{232}Th tailing interference since a large peak width monitor not only the ^{232}Th tailing but also the sides

of the peak which has to be corrected (figure 2c). Recording narrower peaks at half masses allows one to clearly distinguish the ^{232}Th tailing. In the program used for data processing, the parts of the peak that record both peak tailing and ^{232}Th tailing were discarded (figure 4)

3.4 - Isobaric interferences linked to hydride formation

Isobaric interference with hydride $^{232}\text{Th}^1\text{H}$ and $^{235}\text{U}^1\text{H}$ must also be considered for ^{233}Pa and ^{236}U measurements, respectively, (Crain and Alvarado, 1994; Sumiya et al., 1994; Boulyga et al., 2000). Sample introduction methods, uptake rates and nebulizer types are known to affect hydrides generation in the plasma (Crain and Alvarado, 1994; Chiappini et al., 1996; Becker et al., 1999). $^{232}\text{Th}^1\text{H}$ can correspond to up to 0.01% of the ^{232}Th peak with standard pneumatic nebulizers (Hallenbach et al., 1994). The use of membrane desolvation, by which the solvent is removed from the aerosol stream by an argon sweep gas, reduces the hydride formation rate by up to two orders of magnitude for $^{238}\text{U}^1\text{H}$ (Boulyga et al., 2000) and by a factor of seven for $^{232}\text{Th}^1\text{H}$ (Minnich and Houk, 1998). Additionally, small sample uptake rates allowed by microconcentric nebulizers minimize the generation of hydrides. For instance, using a MCN-6000 (Cetac™), Kim et al. (2000) found that hydride formation during U analysis was reduced five-fold leading to a $^{238}\text{U}^1\text{H}/^{238}\text{U}$ ratio value of 1.4×10^{-5} , while Eroglu et al. (1998) found a value of 0.95×10^{-5} for this ratio by using an ultrasonic nebulizer. Choi et al. (2001) found an average value of 0.95×10^{-5} for $^{232}\text{Th}/^{232}\text{Th}^1\text{H}$ by using both a MCN-6000 (Cetac™) and a PFA nebulizer.

Since our operating conditions are similar to that employed by Choi et al. (2001) and Kim et al. (2000), we have extrapolated a value of 1.4×10^{-5} to calculate the hydride contribution to the ^{236}U signal (2.6×10^5 cps) which we used to determine the ^{238}U concentration. Hence, we got $^{235}\text{U} = ^{238}\text{U}/137.88 \approx 1100$ cps and $^{235}\text{U}^1\text{H} \approx 1.4 \times 10^{-5} \times 1100 < 1$ cps, showing that the $^{235}\text{U}^1\text{H}$ contribution was negligible.

Since the measurement of the ^{232}Th peak in the Pa fraction would overflow the ion-counter, a correction based on the value at mass 231.5 was applied (Choi et al.,

2001). This value takes into account both the ^{232}Th tailing and the $^{232}\text{Th}^1\text{H}$ and is 0.5 times the signal at mass 231.5. In our samples it was representing 0.2 to 1 % of the signal at mass 233. Assuming a value of 1.4×10^{-5} for $^{232}\text{Th}^1\text{H}/^{232}\text{Th}$, the hydride $^{232}\text{Th}^1\text{H}$ contribution to mass 233 can be estimated with the $^{232}\text{Th}/^{231}\text{Pa}$ ratios calculated in section 3.3. It is < 100 cps for MD 2138 samples and < 10 cps for ODP 849 samples.

3.5 - Instrumental mass fractionation

Isotopes from the same element are transmitted by a mass spectrometer with an efficiency that varies with the isotope mass. This process, called instrumental mass fractionation, can generate analytical errors during ICP-MS measurements (e.g. Price Russ and Bazan, 1987). Instrumental mass fractionation preferentially affects low masses (Urey, 1947; Tomascak et al., 1999) therefore only small corrections are required in the high mass range of the U-series isotopes. Because of the variable nature of the mass bias, no constant mass discrimination can be applied (Gwiazda et al., 1998 and figure 5). For these measurements, a NBS 960 uranium standard was used as an external mass bias monitor. An external mass fractionation correction was employed because (1) there are no Pa and Th isotopes than can be used for internal mass bias monitoring and (2) internal spiking of U, which is already present in the analyzed samples, would have added to the uncertainty of the measurements. The mass fractionation factor per a.m.u. was assumed to be equal for U, Pa and Th, which is justified by the high mass of the three elements and the small mass range covered by their isotopes. To measure the mass bias we have bracketed each sample and each couple of samples for the ^{232}Th - ^{238}U aliquot, respectively, by NBS 960 measurements. We have assumed a linear variation between the two bracketing standards. The mass fractionation was calculated on the basis of the average NBS 960 value. We have used both a linear and an exponential law to correct for the instrumental mass bias. Differences between the two corrections were found to be less than 0.5 %. Therefore the mass bias correction was performed using (4) (Russell et al., 1978):

$$(^x\text{A}/^y\text{A})_{\text{corr}} = (^x\text{A}/^y\text{A})_{\text{meas}} \cdot (1 + |x-y| \cdot f) \quad (4)$$

where $(^x\text{A}/^y\text{A})_{\text{corr}}$ is the mass bias corrected ratio of isotopes ^xA (mass x) and ^yA (mass y), $(^x\text{A}/^y\text{A})_{\text{meas}}$ is the measured ratio of isotopes ^xA and ^yA , and f is the mass fractionation factor per a.m.u. calculated from (5).

$$f = \frac{1}{\Delta M} \times \left[\frac{(^{238}\text{U}/^{235}\text{U})_{\text{ave}}}{(^{238}\text{U}/^{235}\text{U})_{\text{nat}}} - 1 \right] \quad (5)$$

where $(^{238}\text{U}/^{235}\text{U})_{\text{ave}}$ is the average value of the ratios in NBS960 measured before and after the sample measurement, $(^{238}\text{U}/^{235}\text{U})_{\text{nat}}$ is the natural value of 137.88, i.e. the value of the NBS standard, and ΔM is the mass difference between ^{235}U and ^{238}U .

f was found to be usually lower than 0.004. The mass fractionation varied between 0.0008 and 0.0043/a.m.u. over 24 hours, i.e., 30 NBS960 measurements. However, the variation between 2 consecutive measurements (i.e. two measurements surrounding 2 samples and 2 blanks) is usually < 0.0005 /a.m.u. and does not exceed 0.0015/a.m.u.. The variations in f over 24 hours of measurements are shown in figure 5. The mass bias correction ranged from 0.1 to 0.5 % for the $^{231}\text{Pa}/^{233}\text{Pa}$ and $^{230}/^{229}\text{Th}$ ratios, and 0.5 to 1 % for the $^{238}\text{U}/^{236}\text{U}$ and $^{232}\text{Th}/^{229}\text{Th}$ ratios. Results in figure 5 show that the mass bias varied by steps, with periods of time of 2 to 4 hours during which variation was < 25 % and jumps occurring in less than 1 hour during which f variations could be > 100 %. These results clearly demonstrate the necessity of an accurate and frequent mass bias measurement for ^{231}Pa and ^{230}Th determination by SF-ICP-MS.

4 - Replicate analyses

Replicate analyses were performed for seven samples (table 6). The average overall reproducibility (2σ standard error) was 4.5% for the $(^{231}\text{Pa}/^{230}\text{Th})_{\text{xs},0}$ ratio, < 3.5 % for $(^{230}\text{Th})_{\text{xs},0}$, < 7 % for $(^{231}\text{Pa})_{\text{xs},0}$, and < 3 % for (^{238}U) . The bad reproducibility on the (^{232}Th) activities is likely to arise from the very low detrital content in the sediment analyzed for this study, inducing very low values of ^{232}Th .

5 - Data processing

Data acquisition consisted of 30 consecutive runs over the entire mass range, which averaged 30 passes each. The time-resolved raw data recorded by the ICP-MS software were loaded into a Matlab[®] (The MathWorks, Inc.) program. Count rates average and standard deviations were automatically calculated on the mass range corresponding to the flat top of each peak, with the same peak width for every mass, and every half mass, respectively. The program allows the user to have a graphical control on each step of the data regression. Outliers resulting from electronic interferences were removed. A point was determined as an outlier when its residual was more than three standard deviations from the mean value of residuals (figure 6). Removal of the outliers was decided by a graphical interface. Then the program subtracted the background and the procedural blank (corrected from the background) for each mass. The ^{232}Th (corrected from the background) tailing is then removed. The peak width taken into account for the ^{232}Th tailing correction can be reduced by the user to avoid taking into account the tailing of the mass to correct (figure 2). Isotopic ratios were calculated for each of the consecutive runs and corrected for the instrumental mass fractionation. The reported internal precision (table 7) is twice the standard deviation on the ratio divided by the square root of the number of measurements, i.e. typically 30 consecutive runs which are averages of 30 passes each. ^{230}Th , ^{231}Pa , ^{232}Th , and ^{238}U were calculated using a standard isotope dilution equation which included the correction from the spikes contribution to the ratio.

5.1 - Contaminations due to the chemical procedures and samples spiking

Although the measured isotopes are not common in materials and instruments used in the laboratory, the chemical procedure can contaminate the samples through the addition of the reagents, the contact with resins or containers like beakers. The contamination arising from the overall chemical procedure, referred hereafter as procedural blank, was measured for each batch of sample preparation. Typical values are reported in table 5. Procedural blanks usually represent less than 0.8 % of the signal. The

resin can contribute significantly to the blank and therefore great care must be taken to clean the resin thoroughly prior to sample processing.

Another factor of sample contamination arise from the spiking because spikes are not free of other isotopes and elements. In particular, the solution of ^{232}Th used to produce ^{233}Pa also contains small amounts of ^{230}Th which produces ^{231}Pa by neutron capture. The $^{231}\text{Pa}/^{233}\text{Pa}$ ratio measured in ^{233}Pa was 2×10^{-4} , three times lower than the value reported by Bourdon et al. (1999). The ^{231}Pa contamination of the sample by this bias was only 0.05-0.2 fg, i.e. 0.02-0.08 ‰ of the ^{231}Pa signal and therefore negligible. In each spike, the potential contribution on each mass was recorded by measuring the ratio of the spike mass to the other masses (table 8). When the ratio in the spike was more than 5×10^{-4} , a correction was applied.

5.2 - Corrections for the contribution of the detrital (det) and the authigenic (auth) fractions of the sediment

The corrections were made according to equations (8) and (9) for ^{230}Th and ^{231}Pa respectively. The following equations are written in activities and activity ratios:

$$^{230}\text{Th}_{\text{xs}} = ^{230}\text{Th}_{\text{meas}} - ^{230}\text{Th}_{\text{det}} - ^{230}\text{Th}_{\text{auth}} \quad (7)$$

$$^{230}\text{Th}_{\text{xs}} = ^{230}\text{Th}_{\text{meas}} - (^{232}\text{Th}_{\text{meas}} \cdot R_{\text{lith}}) - (^{234}\text{U}_{\text{auth}} \cdot (1 - e^{-\lambda_{230}\text{Th} \cdot t})) \quad (8)$$

$$^{231}\text{Pa}_{\text{xs}} = ^{231}\text{Pa}_{\text{meas}} - ((^{235}\text{U}/^{238}\text{U})_{\text{sw}} \cdot ^{232}\text{Th}_{\text{meas}} \cdot R_{\text{lith}}) - (^{235}\text{U}_{\text{auth}} \cdot (1 - e^{-\lambda_{231}\text{Pa} \cdot t})) \quad (9)$$

with: $^{234}\text{U}_{\text{auth}} = (^{234}\text{U}/^{238}\text{U})_{\text{sw}} \cdot (^{238}\text{U}_{\text{meas}} - R_{\text{lith}} \cdot ^{232}\text{Th}_{\text{meas}})$

$$^{235}\text{U}_{\text{auth}} = (^{235}\text{U}/^{238}\text{U})_{\text{sw}} \cdot (^{238}\text{U}_{\text{meas}} - R_{\text{lith}} \cdot ^{232}\text{Th}_{\text{meas}})$$

where: $R_{\text{lith}} = 0.8 \pm 0.2$ is the average ($^{238}\text{U}/^{232}\text{Th}$) activity ratio in the lithogenic fraction of the sediment,

$$(^{234}\text{U}/^{238}\text{U})_{\text{sw}} = 1.144 \text{ is the average } (^{234}\text{U}/^{238}\text{U}) \text{ activity ratio in the seawater,}$$

$$(^{235}\text{U}/^{238}\text{U})_{\text{sw}} = 0.046 \text{ is the average } (^{235}\text{U}/^{238}\text{U}) \text{ activity ratio in the seawater,}$$

where t is the age of sediment deposition determined with an independent chronometer, like $\delta^{18}\text{O}$ or ^{14}C .

Conclusion

We have evaluated the various corrections and contributions to the signals of ^{231}Pa and ^{230}Th in order to reach an internal precision of the order of 1.5 % on the $(^{231}\text{Pa}/^{230}\text{Th})_{\text{xs},0}$ ratio with a high sample throughput. This represents a significant improvement compared to previous methods of measurement by alpha and beta-spectrometry. Three deep-sea sediment downcore profiles have been obtained using ^{231}Pa and ^{230}Th measurements by SF-ICP-MS. The downcore profiles show a remarkably good internal coherency. The technique has allowed us to quickly measure two downcore profiles, over 85,000 years, with an average resolution of 1 sample per 2.5 kyr, and 1 sample per 5 kyr, respectively. The measurement of ^{231}Pa and ^{230}Th by SF-ICP-MS is a valuable technique. It was also developed for seawater (Choi et al., 2001) where it shows highly promising results. This method has the potential to be used for measurements of U-series disequilibria ($^{231}\text{Pa}/^{235}\text{U}$ and $^{230}\text{Th}/^{238}\text{Th}$) in young volcanic rocks.

Acknowledgements: We thank the WHOI ICP Facility for use of the Finnigan MAT Element I sector field inductively coupled plasma mass spectrometer (SF-ICP-MS). S. P. gratefully acknowledges the support of the CNRS-NSF, the Eurodoc program of the Région Rhône-Alpes, and the Geology and Geophysics Dept (WHOI).

References

- Albert, P., Nuclear methods in trace and ultra-trace analysis: past experiences and future possibilities, *Pure Appl. Chem.* **54**, 689-713, 1982.
- Anderson, R. F., M. P. Bacon, and P. G. Brewer, Removal of ^{230}Th and ^{231}Pa from the open ocean, *Earth Planet. Sci. Lett.* **62**, 7-23, 1983a.
- Anderson, R. F., M. P. Bacon, and P. G. Brewer, Removal of ^{230}Th and ^{231}Pa from the ocean margins, *Earth Planet. Sci. Lett.* **66**, 73-90, 1983b.
- Anderson, R. F., and A. P. Fleer, Determination of natural actinides and plutonium in marine particulate material, *Anal. Chem.* **54**, 1142-1147, 1982.
- Bacon, M. P., Tracers of chemical scavenging in the ocean: boundary effects and large-scale chemical fractionation, *Philos. Trans. R. Soc. London, Ser. A* **325**, 147-160, 1988.
- Bacon, M. P., Glacial to interglacial changes in carbonate and clay sedimentation in the Atlantic Ocean estimated from ^{230}Th measurements, *Isot. Geosci.* **2**, 97-111, 1984.
- Bacon, M. P., and R. F. Anderson, Distribution of thorium isotopes between dissolved and particulate forms in the deep sea, *J. Geophys. Res.* **87**, C3, 2045-2056, 1983.
- Bacon, M. P., and J. N. Rosholt, Accumulation rates of ^{230}Th , ^{231}Pa , and some transition metals on the Bermuda Rise, *Geochim. Cosmochim. Acta* **46**, 651-666, 1982.
- Becker, J. S., S. V. Soman, K. L., Sutton, J. A., Caruso, and H.-J. Dietze, Determination of long-lived radionuclides by inductively coupled plasma quadrupole mass spectrometry using different nebulizers, *J. Anal. At. Spectr.* **14**, 933-937, 1999.
- Bernat, M., and E. D. Goldberg, Thorium isotopes in the marine environment, *Earth Planet. Sci. Lett.* **5**, 308-312, 1969.
- Boulyga, S. F., J. S. Becker, J. L. Matusevitch, and H. -J. Dietze, Isotope ratio measurements of spent reactor uranium in environmental samples by using inductively coupled plasma mass spectrometry, *Int. J. Mass Spectr.* **203**, 143-154, 2000.

- Bourdon, B., J.-L. Joron, and C. J. Allegre, A method for ^{231}Pa analysis by thermal ionization mass spectrometry in silicate rocks, *Chem. Geol.* **157**, 147-151, 1999.
- Bourdon, B., J.-L. Joron, C. Claude-Ivanaj, and C. J. Allègre, U-Th-Pa-Ra systematics for the Grande Comore volcanics: melting processes in an upwelling plume, *Earth Planet. Sci. Lett.* **164**, 119-133, 1998.
- Chen, J. H., R. L. Edwards, and G. J. Wasserburg, ^{238}U - ^{234}U - ^{232}Th in seawater. *Earth Planet. Sci. Lett.* **80**, 241-251, 1986.
- Chiappini, R., J.-M. Taillade, and S. Brébion, Development of a High-sensitivity Inductively Coupled Plasma Mass Spectrometer for Actinide Measurement in the Femtogram Range, *J. Anal. At. Spectr.* **7**, 497-504, 1996.
- Cochran, J.K., The oceanic chemistry of the uranium- and thorium-series nuclides. In *Uranium-series disequilibrium: Applications to Earth, marine, and environmental Sciences*, Ivanovich, M., and R. S. Harmon (Eds), Clarendon Press, Oxford, U.K., 334-395, 1992.
- Crain, J., and J. Alvarado, Hydride interference on the determination of minor actinide isotopes by inductively coupled plasma mass spectrometry, *J. Anal. At. Spectr.* **9**, 1223-1227, 1994.
- Edmonds, H. N., S. B. Moran, J. A. Hoff, J. N. Smith, and R. L. Edwards, Protactinium-231 and thorium-230 abundances and high scavenging rates in the western Arctic Ocean, *Science* **280**, 405-407, 1998.
- Edwards, R. L., H. Cheng, M. T. Murrell, and S. J. Goldstein, Protactinium-231 dating of carbonates by thermal ionization mass spectrometry: Implications for Quaternary climate change, *Science* **276**, 782-786, 1997.
- Eroglu, A. E., C. W. McLeod, K. S. Leonard, and D. McCubbin, Determination of plutonium in seawater using co-precipitation and inductively coupled plasma mass spectrometry with ultrasonic nebulization, *Spectrochim. Acta B* **53**, 1221-1233, 1998.
- Field, M. P., and R. M. Sherrell, Magnetic sector ICPMS with desolvating micronebulization: Interference-free subpicogram determination of rare earth elements in natural samples, *Anal. Chem.* **70**, 4480-4486, 1998.

- Firestone, R. B., *Table of isotopes*, 8th Edition, Shirley, V.S. (Ed), John Wiley & Sons, New York, U.S.A., 1996.
- Fleer, A. P., and M. P. Bacon, Notes on some techniques of marine particle analysis used at WHOI. In *Marine Particles: Analysis and Characterization*, Hurd, D. C., and D. W. Spencer (Eds), *Geophys. Monograph.* **63**, AGU, 223-226, 1991.
- François, R., M. P. Bacon, J. Bullister, A. P. Fleer, S. Brown-Leger, D. Wisegarver, Constraining deep water circulation and mixing in the Atlantic from ^{230}Th and ^{231}Pa seawater profiles, *Ocean Science Meeting abstract*, San Antonio, 2000.
- François, R. F., M. A. Altabet, E.-F. Yu, D. M. Sigman, M. P. Bacon, M. Frank, G. Bohrmann, G. Bareille, and L. D. Labeyrie, Water column stratification in the Southern Ocean contributed to the lowering of glacial atmospheric CO_2 , *Nature* **389**, 929-935, 1997.
- François, R., M. P. Bacon, M. A. Altabet, and L. D. Labeyrie, Glacial/interglacial changes in sediment rain rate in the Indian sector of Subantarctic water as recorded by ^{230}Th , ^{231}Pa , U, and ^{15}N , *Paleoceanography* **8**, 611-629, 1993.
- François, R., Bacon, M. P., and D. O. Suman, Thorium-230 profiling in deep-sea sediments: High-resolution records of flux and dissolution of carbonate in the equatorial Atlantic during the last 24,000 years, *Paleoceanography* **5**, 761-787, 1990.
- Frank, M., R. Gersonde, and A. Mangini, Sediment redistribution, $^{230}\text{Th}_{\text{ex}}$ - normalization and implications for the reconstruction of particle flux and export paleoproductivity. In *Use of proxies in Paleoceanography: Examples from the South Atlantic*, Fischer, G., and G. Wefer (Eds), Springer-Verlag, Berlin Heidelberg, Germany, 410-426, 1999.
- Frank, M., J.-D. Eckhardt, A. Eisenhauer, P. W. Kubik, B. Dittrich-Hannen, M. Segl, and A. Mangini, Beryllium 10, Thorium 230, and Protactinium 231 in Galapagos microplate sediments: implications of hydrothermal activity and paleoproductivity changes during the last 100,000 years, *Paleoceanography* **9**, 559-578, 1994.
- Guillaumont R., G. Bousieres, and R. Muxart, Chimie du protactinium, 1. solution aqueuses de protactinium penta- et tétravalent, *Actinides Rev.* **1**, 135-163, 1968.

- Goldstein, S. J., M. T. Murell, and R. W. Williams, ^{231}Pa and ^{230}Th chronology of mid-ocean ridge basalts, *Earth Planet. Sci. Lett.* **115**, 151-159, 1993.
- Gwiazda, R., D. Woolard, and D. Smith, Improved lead isotope ratio measurements in environmental and biological samples with a double focussing magnetic sector inductively coupled plasma mass spectrometer (ICP-MS), *J. Anal. At. Spectr.* **13**, 1233-1238, 1998.
- Hallenbach, M., J. Grohs, S. Mamich, and M. Kroft, Determination of technetium-99, thorium-230 and uranium-234 in soils by inductively coupled plasma mass spectrometry using flow injection preconcentration, *J. Anal. At. Spectr.* **9**, 927-933, 1994.
- Henderson, G. M., and N. C. Slowey, Evidence against northern-hemisphere forcing of the penultimate deglaciation from U-Th dating, *Nature* **402**, 61-66, 2000.
- Huh, C.-A., and T. M. Beasley, Profiles of dissolved and particulate thorium isotopes in the water column of coastal Southern California, *Earth Planet. Sci. Lett.* **85**, 1-10, 1987.
- Kadko, D., a detailed study of some uranium series nuclides at an abyssal hill area near the East Pacific Rise at $8^{\circ}45'\text{N}$, *Earth Planet. Sci. Lett.* **51**, 115-131, 1980.
- Kim, C.-S., C.-K. Kim, J.-I. Lee, and K.-J. Lee, Rapid determination of Pu isotopes and atom ratios in small amounts of environmental samples by an on-line pre-treatment system and isotope dilution high resolution inductively coupled plasma mass spectrometry, *J. Anal. At. Spectr.* **15**, 247-255, 2000.
- Kim, C.-K., R. Seki, S. Morita, S. I. Yamasaki, A. Tsumura, Y. Takaku, Y. Igarashi, and M. Yamamoto, Application of a high resolution inductively coupled plasma mass spectrometer to the measurement of long-lived radionuclides, *J. Anal. At. Spectr.* **6**, 205-209, 1991.
- Kumar, N., R. F. Anderson, R. A. Mortlock, P. N. Froelich, P. Kubik, B. Dittrich-Hannen, and M. Suter, Increased biological productivity and export production in the glacial Southern Ocean, *Nature* **378**, 675-680, 1995.

- Kumar, N., G. Gwiazda, R. F. Anderson, and P. N. Froelich, $^{231}\text{Pa}/^{230}\text{Th}$ ratios in sediments as a proxy for past changes in the Southern Ocean productivity, *Nature* **362**, 45-48, 1993.
- Lao, Y., R. F. Anderson, and W. S. Broecker, Boundary scavenging and deep-sea sediment dating: constraints from excess ^{230}Th and ^{231}Pa , *Paleoceanography* **7**, 783-798, 1992.
- Layne, G. D., and Sims, K. W., Analysis of $^{232}\text{Th}/^{230}\text{Th}$ in volcanic rocks by Secondary Ionization Mass Spectrometry, *Int. J. Mass Spectr.* **203**, 187-198, 2000.
- Luo, S., T.-L. Ku, M. Kusakabe, J. K. B. Bishop, and Y.-L. Yang, Tracing particle cycling in the upper ocean with ^{230}Th and ^{228}Th : An investigation in the equatorial Pacific along 140°W , *Deep Sea Res. B* **42**, 805-829, 1995.
- Mangini, A., and U. Kühnel, Depositional history in the Clarion-Clipperton zone during the last 250,000 years: ^{230}Th and ^{231}Pa methods, *Geol. Jahrbuch* **87**, 105-121, 1987.
- Mangini, A., and C. Sonntag, ^{231}Pa dating of deep-sea cores via ^{227}Th counting, *Earth Planet. Sci. Lett.* **37**, 251-256, 1977.
- Marcantonio, F., R. F. Anderson, S. Higgins, M. Stute, and P. Schloesser, Sediment focusing in the central equatorial Pacific Ocean, *Paleoceanography* **16**, 260-267, 2001.
- Marchal, O., R. François, T. F. Stocker, and F. Joos, Ocean thermohaline circulation and sedimentary $^{231}\text{Pa}/^{230}\text{Th}$ ratio, *Paleoceanography* **15**, 625-641, 2000.
- Minnich, M. G., and R. S. Houk, Comparison of cryogenic and membrane desolvation for attenuation of oxide, hydride and hydroxide ions and ions containing chlorine in inductively coupled plasma mass spectrometry, *J. Anal. At. Spectr.* **13**, 167-174, 1998.
- Moran, S. B., M. A. Charette, J. A. Hoff, R. L. Edwards, and W. M. Landing, Distribution of ^{230}Th in the Labrador Sea and its relation to ventilation, *Earth Planet. Sci. Lett.* **150**, 151-160, 1997.
- Niu, H. S., and R. S. Houk, Fundamental aspects of ion extraction in ICP-MS, *Spectrochim. Acta B* **51**, 779-815, 1996.

- Nozaki, Y., and T. Nakanishi, ^{231}Pa and ^{230}Th profiles in the open ocean water column, *Deep Sea Res.* **32**, 1209-1220, 1985.
- Nozaki, Y., Y. Horibe, and H. Tsubota, The water column distributions of thorium isotopes in the western North Pacific, *Earth Planet. Sci. Lett.* **54**, 203-216, 1981.
- Paytan, A., M. Kastner, and F. Chavez, Glacial to interglacial fluctuations in productivity in the equatorial Pacific as indicated by marine barite, *Science* **274**, 1355-1357, 1996.
- Pichat, S., K. W. Sims, R. François, J. F. McManus, and F. Albarède, Lower biological productivity during glacial periods in the equatorial Pacific as derived from $(^{231}\text{Pa}/^{230}\text{Th})_{\text{xs},0}$ measurements in deep-sea sediments, in preparation.
- Choi, M. S., R. François, K. Sims, M. P. Bacon, S. Brown-Leger, A. P. Fler, L. A. Ball, D. Schneider, and S. Pichat, Rapid determination of ^{230}Th and ^{231}Pa in seawater by desolvated micro-nebulization Inductively Coupled Plasma magnetic sector mass spectrometry, *Marine Chem.* **76**, 99-112, 2001.
- Pickett, D. A., and M. T. Murrell, Observation of $^{231}\text{Pa}/^{235}\text{U}$ disequilibrium in volcanic rocks, *Earth Planet. Sci. Lett.* **148**, 259-271, 1997.
- Pickett, D. A., M. T. Murrell, and R. W. Williams, Determination of femtogram quantities of protactinium in geologic samples by thermal ionization mass spectrometry, *Anal. Chem.* **66**, 1044-1049, 1994.
- Price Russ III, G., and J. M. Bazan, Isotopic ratio measurements with an inductively coupled plasma source mass spectrometer, *Spectrochim. Acta B* **42**, 49-62, 1987.
- Rodushkin, I., P. Lindahl, E. Holm, and P. Roos, Determination of plutonium concentrations and isotope ratios in environmental samples with a double-focusing sector field ICP-MS, *Nucl. Instr. Meth. Phys. Res. A* **423**, 472-479, 1999.
- Russell, W. A., D. A. Papanastassiou, and T. A. Tombrello, Ca isotope fractionation on the earth and other solar system materials, *Geochim. Cosmochim. Acta* **42**, 1075-1090, 1978.
- Shaw, T. J., and R. François, A fast and sensitive ICP-MS assay for the determination of ^{230}Th in marine sediments, *Geochim. Cosmochim. Acta* **55**, 2075-2078, 1991.

- Shimmield, G. B., and N. B. Price, The scavenging of U, ^{230}Th , and ^{231}Pa during pulsed hydrothermal activity at 20°S, East Pacific Rise, *Geochim. Cosmochim. Acta* **52**, 669-677, 1988.
- Sims, K. W. W., D. J. DePaolo, M. T. Murrell, W. S. Baldrige, S. Goldstein, D. Clague, and M. Jull, Porosity of the melting zone and variations in the solid mantle upwelling rate beneath Hawaii: Inferences from ^{238}U - ^{230}Th - ^{226}Ra and ^{235}U - ^{231}Pa disequilibria, *Geochim. Cosmochim. Acta* **63**, 4119-4138, 1999.
- Stephens, M. P., and D. C. Kadko, Glacial-Holocene calcium carbonate dissolution at the central equatorial Pacific seafloor, *Paleoceanography* **12**, 797-804, 1997.
- Suman, D. O., and M. P. Bacon, Variations in Holocene sedimentation in the north American basin determined from Th-230 measurements, *Deep Sea Res.* **36**, 869-878, 1989.
- Sumiya, S., S. Morita, K. Tobita, and M. Kurabayashi, Determination of technetium-99 and neptunium-237 in environmental samples by inductively coupled plasma mass spectrometry, *J. Rad. Nucl. Chem.* **177**, 149-164, 1994.
- Tomascak, P. B., R. W. Carlson, and S. B. Shirey, Accurate and precise determination of Li isotopic compositions by multi-collector sector ICP-MS, *Chem. Geol.* **158**, 145-154, 1999.
- Urey, H. C., The thermodynamics of isotopic substances, *J. Chem. Soc.*, 562-581, 1947.
- Walter, H. J., M. M. Rutgers van der Loeff, and R. François, Reliability of the $^{231}\text{Pa}/^{230}\text{Th}$ activity ratio as a tracer for bioproductivity of the ocean. In *Use of proxies in Paleoceanography: Examples from the South Atlantic*, Fischer, G., and G. Wefer (Eds), Springer-Verlag, Berlin Heidelberg, Germany, 393-408, 1999.
- Walter, H. J., M. M. Rutgers van der Loeff, and H. Hoeltzen, Enhanced scavenging of ^{231}Pa relative to ^{230}Th in the South Atlantic south of the Polar front: Implications for the use of the $^{231}\text{Pa}/^{230}\text{Th}$ ratio as a paleoproductivity proxy, *Earth Planet. Sci. Lett.* **149**, 85-100, 1997.

Yu, E. F., R. François, and M. P. Bacon, Similar rates of modern and last-glacial ocean thermohaline circulation inferred from radiochemical data, *Nature* **379**, 689-694, 1996.

Yu, E. F., Variations in the particulate flux of ^{230}Th and ^{231}Pa and paleoceanographic applications of the $^{231}\text{Pa}/^{230}\text{Th}$ ratio, Ph.D. thesis, MIT-WHOI, MA, U.S.A., 269 pp., 1994.

Tables

depth* (cm)	$^{231}\text{Pa}_{\text{xs}}$ (dpm/g)	standard deviation
2 - 4	4.48 ± 0.25	5.6%
7 - 10	4.08 ± 0.20	4.9%
15 - 20	1.43 ± 0.10	7.0%
25 - 30	0.87 ± 0.17	19.5%
35 - 40	0.04 ± 0.12	300%
depth** (cm)	$^{231}\text{Pa}_{\text{xs}}$ (dpm/g)	standard deviation
5 - 7	3.65 ± 0.20	5.50%
30 - 32	1.68 ± 0.15	8.90%
75 - 77	1.55 ± 0.08	5.10%
100 - 102	1.15 ± 0.09	7.80%
125 - 127	0.76 ± 0.55	72%

Table 1 - Precision of the ^{231}Pa measurements deduced from the β -emission of its ^{227}Th daughter. The standard deviation is based on 1σ counting statistics. The precision decreases rapidly with depth. * data from core Valdivia 10127 (13°42' N 151°40'W 5700 m water depth) (Mangini and Sonntag, 1977). ** data from core 1M17 14P (8°45' N 104°00'W ~ 3000 m water depth) (Kadko, 1980).

Power (W)	(W)	1300-1375
Gas (L/min)	<u>ICP-MS</u>	
	Cool	13.1 to 13.5
	Auxiliary	1.1 to 1.5
	Sample	1.16 to 1.28
	<u>MCN-6000</u>	
	Sweep (Ar)	2.85 to 3.15
	Nitrogen (mL/min)	10 to 20
Lenses (V)	Extraction	-2000
	Focus	-775 to -910
	X-deflection	5 to 11.5
	Y-deflection	-5.3 to -7.9
	Shape	85.2 to 96

Table 2 - Operating parameters for sector type ICP-MS used for sediment samples measurements.

^{231}Pa measurements					
mass	230.5	231	231.5	233	236
scanned mass range	230.39 - 230.61	230.98 - 231.09	231.39 - 231.61	233.98 - 233.09	236.00 - 236.11
sample time (ms)	2	2	2	2	2
samples per peak	150	200	150	200	200
^{230}Th measurements					
mass	229	229.5	230	230.5	231.5
scanned mass range	229.00 - 229.06	229.42 - 229.58	230.00 - 230.06	230.42 - 230.58	231.44 - 231.56
sample time (ms)	2	2	2	2	2
samples per peak	200	100	200	100	100
NBS 960 measurements					
mass	235	238			
scanned mass range	234.99 - 235.11	238.99 - 238.11			
sample time (ms)	2	2			
samples per peak	200	200			
$^{233}\text{U}/^{236}\text{U}$ measurements (U from the last Pa column)					
mass	232.5	233	236		
scanned mass range	232.42 - 232.58	233.01 - 233.07	236.02 - 236.08		
sample time (ms)	1	1	1		
samples per peak	100	200	200		
^{232}Th and ^{238}U measurements (aliquot B)					
mass	229	232	235	236	238
scanned mass range	229.01 - 229.05	232.02 - 232.06	235.02 - 235.06	236.03 - 236.07	238.03 - 238.07
sample time (ms)	2	2	2	2	2
samples per peak	150	150	150	150	150

Table 3 - Scanning parameters for the sector type ICP-MS (Finnigan MAT Element I) for the different mass measurements.

spike	^{229}Th	^{233}Pa	^{236}U
std err. 2σ level	1%	< 1%	0.3%

Table 4 - Spike calibration typical standard error (std err.) calculated at 2σ level, based on the replicate analyses performed during the downcore sediment samples study.

²³¹Pa measurements					
	230.5	231	231.5	233	236
background noise	< 0.1	< 1	1	< 2	2
procedural blank	n.m.	< 10	n.m.	< 20	(a)
sample	6	4,250	45	2,500	280
²³⁰Th measurements					
	229	229.5	230	230.5	231.5
background noise	< 10	< 0.2	4	< 1	< 1
procedural blank	< 150	n.m.	< 200	n.m.	n.m.
sample	500,000	900	125,000	2,200	15,500
NBS 960 measurements					
	235	238			
background noise	1.5	110			
standard ^(b)	17,500	2,400,000			
²³³U/²³⁶U measurements (U from the last Pa column)					
	232.5	233	236		
background noise	< 0.2	< 0.5	5		
procedural blank	n.m.	< 5	n.m.		
sample	100	50	28,000		
²³²Th and ²³⁸U measurements (aliquot B)					
	229	232	235	236	238
background noise	70	6,500	n.u.	100	200 to 2000 ^(d)
sample ^(c)	400,000	300,000	n.u.	2,600,000	1,500,000

Table 5 - Typical number of counts for the background noise, the procedural blanks, and the sample signal corrected for background, procedural blank, ²³²Th tailing and spikes contribution (cps). For each batch of samples two procedural blanks were analyzed. The pairing blanks were always consistent within 10%. ^(a) the procedural blank measured at mass 236 in the last Pa elution range from 5 to 1000 cps (12 procedural blank measurements have been made). n.m.: not measured, and n.u.: not used for the purpose of our measurements. For ^(b) and ^(c) no procedural blank correction were applied. ^(b) is a standard, i.e. there is no chemical procedure involved. For ^(c) the procedural blank contribution is likely to be negligible in view of the high signal recorded. ^(d) Higher background are monitored when using an autosampler, i.e., when the tubes rinsing is not controlled by the operator before each sample measurement (see also figure 4).

sample	# of replicates	$(^{231}\text{Pa}/^{230}\text{Th})_{\text{xs},0}$		$(^{231}\text{Pa})_{\text{xs},0}$ (dpm/g)		$(^{230}\text{Th})_{\text{xs},0}$ (dpm/g)		(^{238}U) (dpm/g)		(^{232}Th) (dpm/g)	
		mean	% se (2σ)	mean	% se (2σ)	mean	% se (2σ)	mean	% se (2σ)	mean	% se (2σ)
MD2138-08	3	0.118	2.9	0.43	4.0	3.71	2.0	1.67	1.5	0.23	3.2
MD2138-20	3	0.120	0.5	0.44	4.1	3.69	4.6	2.74	1.5	0.31	0.7
MD2138-31	3	0.133	1.9	0.48	12.0	3.58	10.9	3.61	2.4	0.3	8.0
MD2138-45	3	0.142	3.6	0.56	4.6	3.95	3.2	3.22	2.8	0.25	28
MD2138-58	2	0.136	8.3	0.63	7.5	4.67	0.8	2.27	3.5	0.33	2.7
MD2138-64	2	0.160	12.2	0.48	12.1	3.00	0.2	2.14	4.2	0.26	2.0
ODP849-162	3	0.100	2.2	0.90	2.0	9.00	1.1	0.12	3.0	0.04	36
ave. se (2σ)		4.5 %		6.6 %		3.2 %		2.7 %		11.5 %	

Table 6 - Reproducibility of the different isotopes and the $(^{231}\text{Pa}/^{230}\text{Th})_{\text{xs},0}$ ratio measurements in deep-sea sediment samples.

isotope	231Pa	233(Pa,U)	230Th	229Th	238U	236U	232Th	229Th
internal precision (2σ)	0.35	0.35	0.35	0.35	0.2	0.2	0.35	0.35

Table 7- Typical internal precision for the measurement of the different isotopes by sector type ICP-MS obtained during the analysis of deep-sea sediment samples.

spike or standard	isotopic ratio		used to quantify:
$^{229}\text{Th}^{(a)}$	$^{230}/^{229}$ 5.8.E-05	$^{232}/^{229}$ 9.4.E-03	^{230}Th
$^{229}\text{Th}^{(b)}$	$^{232}/^{229}$ 4.3.E-04	$^{238}/^{229}$ 4.9.E-03	$^{232}\text{Th}^{(c)}$
^{233}Pa	$^{231}/^{233}$ 2.0.E-4		^{231}Pa
^{233}U	$^{238}/^{233}$ 3.4.E-05		^{238}U
^{236}U	$^{238}/^{236}$ 6.1.E-03	$^{233}/^{236}$ 1.2.E-05	^{238}U ; ^{233}U
^{238}U	$^{236}/^{238}$ 9.6.E-05		^{236}U

Table 8 - Ratio used to correct for the spikes or standards contribution to the measured isotopes signals. $^{(a)}$ and $^{(b)}$ comes from the same mother solution, but $^{(a)}$ is used to determined the concentration of ^{230}Th in the ^{231}Pa - ^{230}Th aliquot, whereas $^{(b)}$ is used to determined the concentration of ^{232}Th in the ^{232}Th - ^{238}U aliquot. $^{(c)}$ since ^{232}Th and ^{238}U are measured in the same fraction of ^{232}Th - ^{238}U aliquot, the 238/229 ratio has been measured to record the potential contamination of mass 238 by the ^{229}Th spike.

Figures

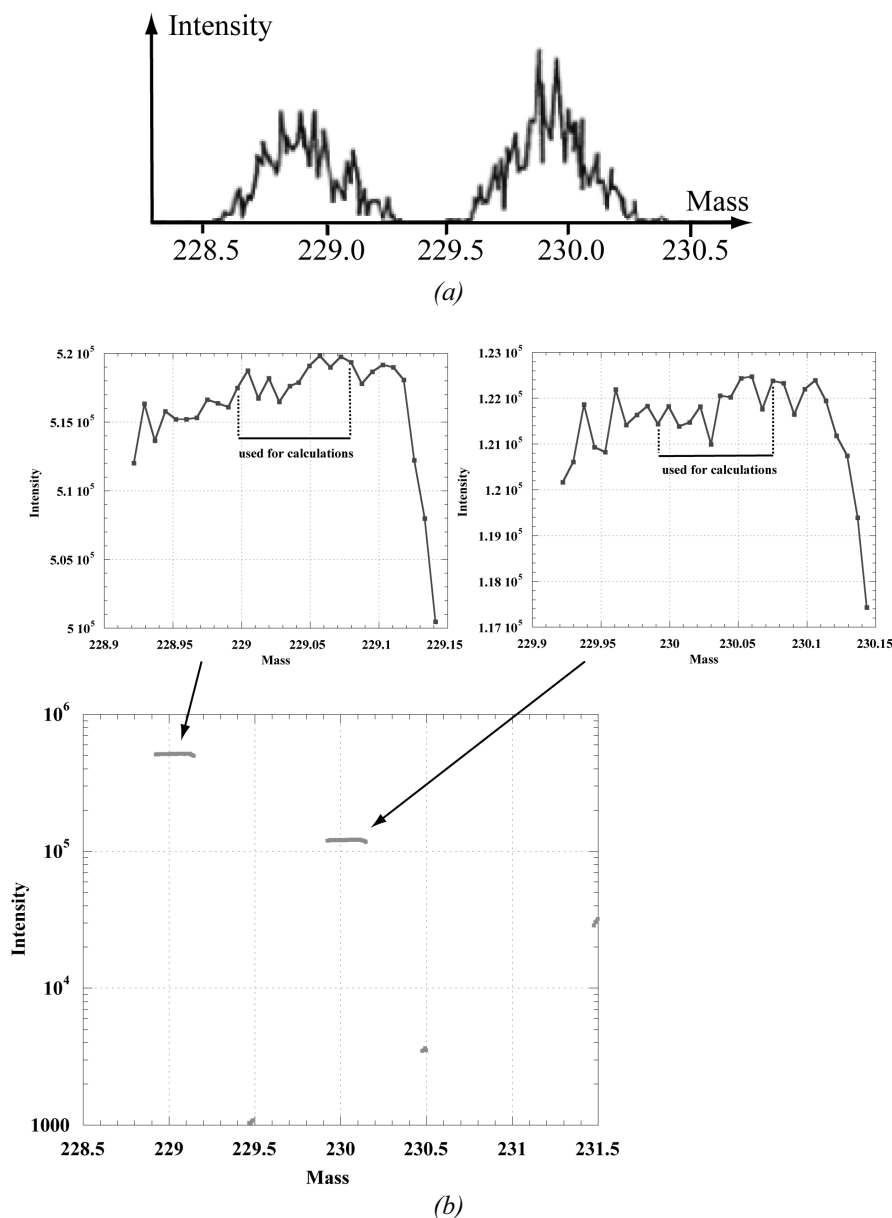


Figure 1 - Spectra obtained with (a) a quadrupole ICP-MS (redrawn after Shaw and François, 1991) (b) a sector type ICP-MS. In (b), the mass range employed for signal intensity calculations, using a Excel-type spreadsheet, are underlined with an horizontal bar. The right side of the 229 and 230 thorium peaks appears clearly in the abrupt signal decrease. The variation in the intensity of the signal on the top part of the peak used for ^{229}Th and ^{230}Th represent less than 0.5 % of the total intensity of the signal.

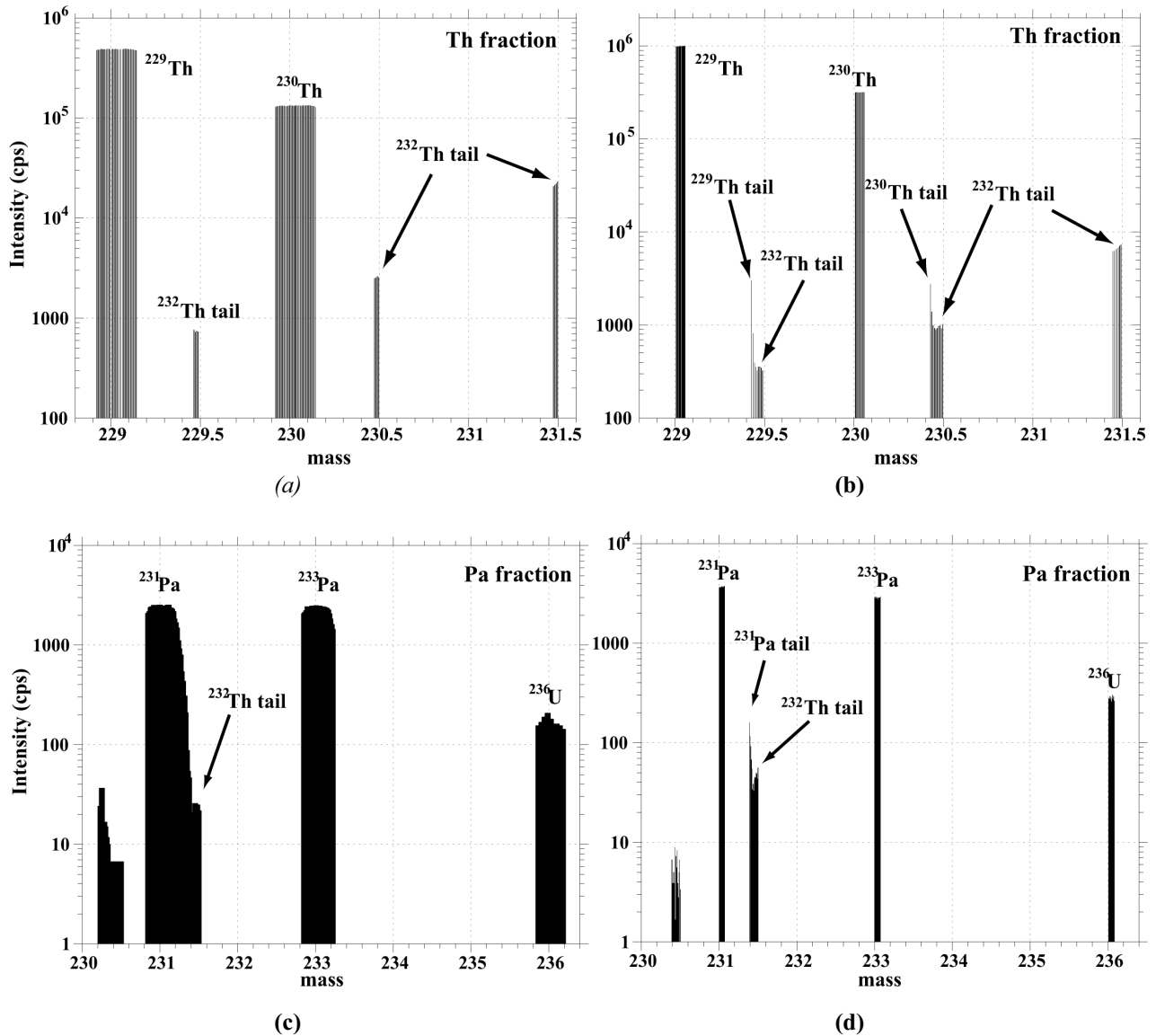


Figure 2 - Sector type ICP-MS spectra for Th and Pa measurements in deep-sea sediments from the western Pacific warm pool (core MD97-2138, $1^{\circ}42'$ N, $146^{\circ}24'$ E, 1900 m water depth). (a) (c) are spectra recorded with the method using wide peaks. In this method the data regression was longer since the sides of the peaks have to be removed in order to select the top flat part of the peaks. Additionally, in (c), the correction for ^{232}Th tailing contribution to the mass 231 peak was less clear than with the use of narrower peaks. (b) (d) are spectra recorded with the method using narrow peaks. Since the half mass peaks are wider, the tailing of the ^{229}Th , ^{230}Th are recorded in (b). Concentrations are calculated by selecting the channels corresponding to the top of the peaks in (a) and (c). In (b) and (d), all the channels for the mass peaks are used.

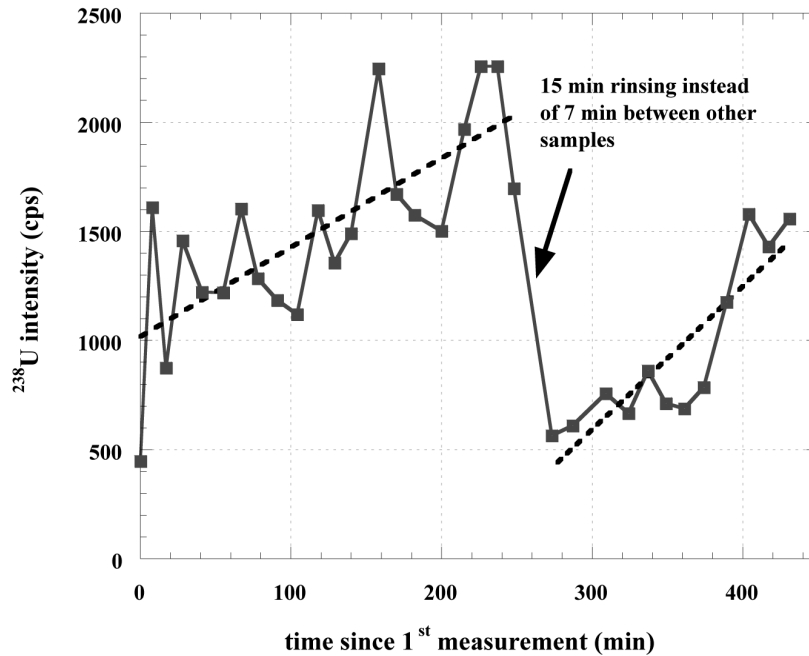


Figure 3 - Evolution of the background noise of the SF-ICP-MS with the input of ^{238}U bearing solution. The increase of the background noise is due to the progressive contamination of the injection system of the ICP-MS, as underlined by the two linear dashed trend lines. This interpretation is confirmed by the four-fold decrease in the background noise as a result of a doubling of the rinsing time between two samples made after 250 min of measurement (shown by the arrow).

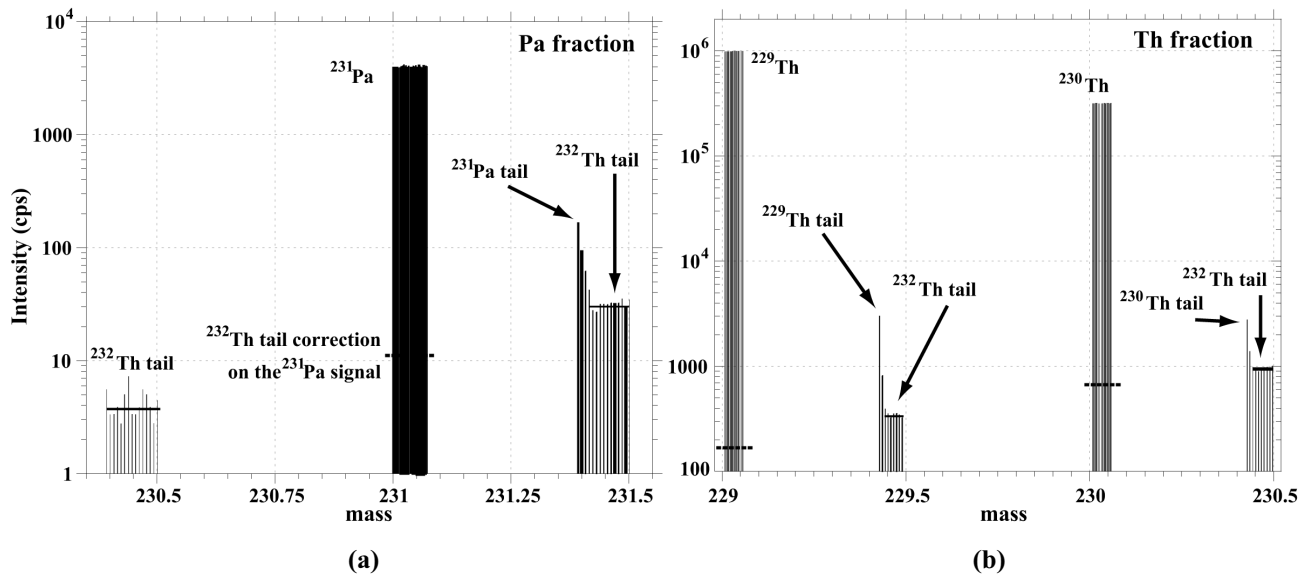


Figure 4 - Correction for the contribution of the ^{232}Th tailing (a) for the Pa fraction and (b) for the Th fraction. In both figures, the signal have been previously corrected for the background contribution. The ^{232}Th tail contribution at mass i ($^{232}\text{Th}_{\text{tail},i}$) is estimated using the following equations: $^{232}\text{Th}_{\text{tail},230} = 0.62 \cdot S(230.5) + 0.38 \cdot S(229.5)$, $^{232}\text{Th}_{\text{tail},229} = 0.4 \cdot S(229.5)$, $^{232}\text{Th}_{\text{tail},231} = (2/3) \cdot S(231.5) + (1/3) \cdot S(230.5)$, where $S(i)$ is the signal at mass i . These equations were determined by fitting masses 231.5, 230.5 and 229.5 with an exponential equation. Although arbitrary, this method allows to regress all the data the same way. $S(i)$ were measured after removing the ^{229}Th , ^{230}Th and ^{231}Pa tail respectively. On the figure, the part of the half mass peaks taken into account for the calculation of the contribution of the ^{232}Th tailing are marked with a horizontal black line. Values of the contribution of the ^{232}Th tailing for mass 229, 230 and 231 are marked on the peak with a horizontal dashed line.

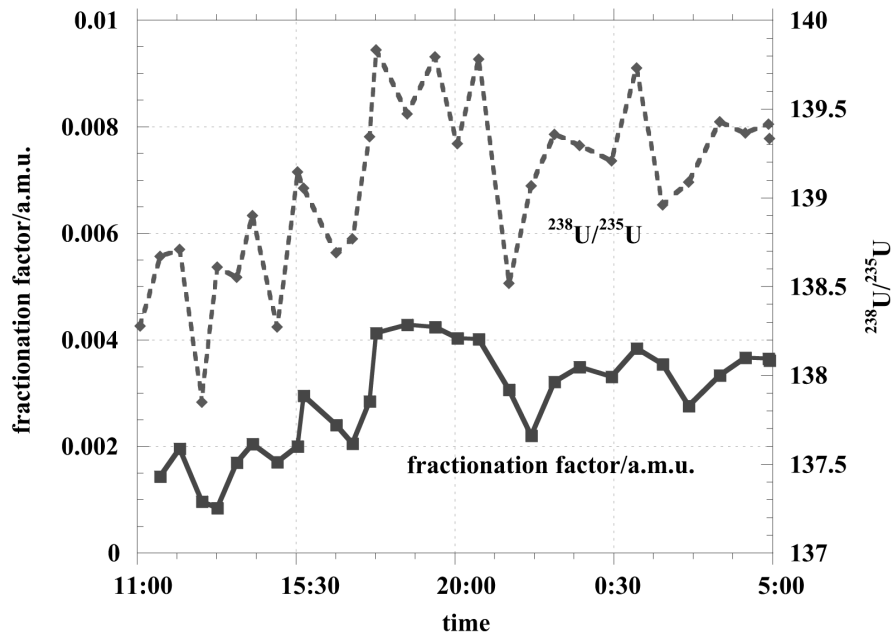


Figure 5 - Variation of the fractionation factor and the measured $^{238}\text{U}/^{235}\text{U}$ ratio values of uranium standard NBS960 over 18 hours of measurement. The $^{238}\text{U}/^{235}\text{U}$ ratio was measured every two samples. The fractionation factor were usually very small ($\sim 0.003/\text{a.m.u.}$) therefore the correction for the instrumental mass fractionation were less than 0.1 % of the signal on the measured isotopes. However, it varies significantly between two measurements supporting the repetitive measurement of an external standard over one day of measurement.

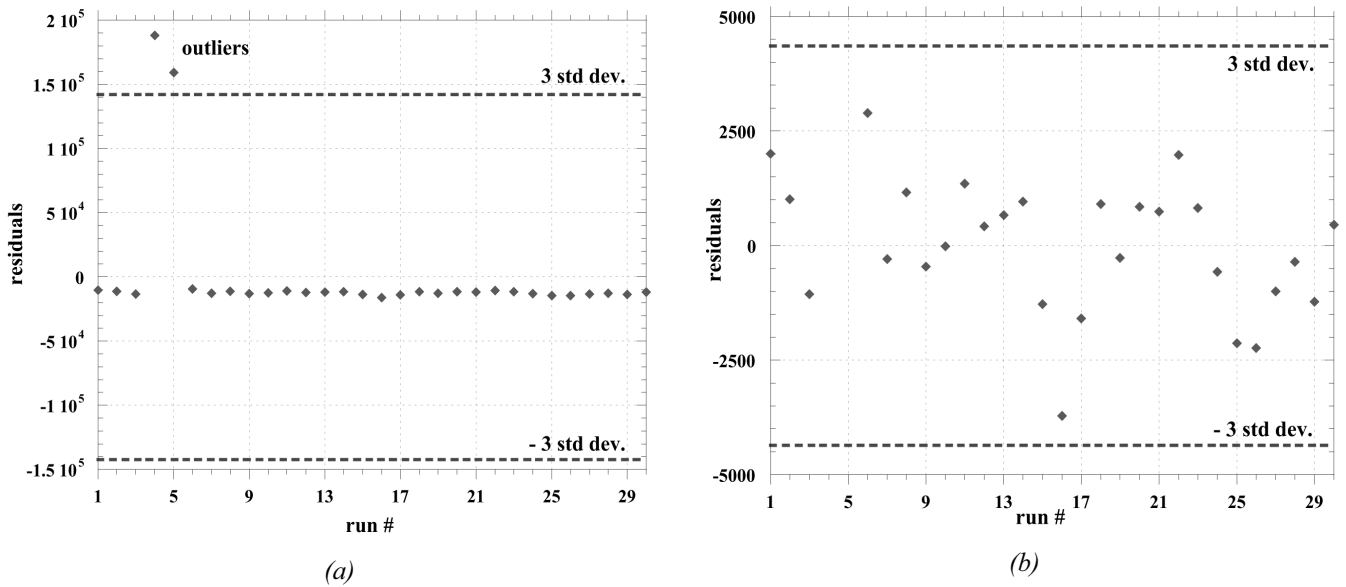


Figure 6 - The importance of tracking outliers is illustrated in this figure. Outliers are tracked with the method of the residuals (see text). In (a) the two outliers are out of the 3 standard deviation area. In (b), the outliers have been removed by the user and a new test has been performed to track remaining outliers. Since all the residuals plot within the new 3 standard deviation area, no other outliers were present. In (a), the intensity of the ^{230}Th signal would have been 73,000 cps whereas in (b) it was 60,000 cps.

6 - Tracer experiments: optimization of the extraction technique for Pa and Th

In the previous paper, tracer experiments were only briefly mentioned. This aspect of the study is further developed hereafter. In this thesis, three different methods of Pa extraction have been tested. The one described in the previous paper, based on anion exchange chromatography on AG1-X8 resin has been inspired and firstly developed by Anderson and Fler (1982), then further optimized by Fler and Bacon (1991), the team of François at the Woods Hole Oceanographic Institution (pers. com.), Sims (pers. com.), Pichat (1997, and previous paper in preparation), and Choi et al. (submitted). Two other methods based on reverse phase extraction chromatography have been investigated. The first one used TRU-Spec[®] (EiChrom technologies, Inc) resin, and the second one used di (2-ethylhexyl) phosphoric acid (HDEHP) coated on Teflon[®] balls. The results of extraction of Pa together with the advantages and the disadvantages for each method are presented in the following sections.

6.1 - Calibration of the column and spike recovery

The calibration of the columns and the recovery of Pa and Th were monitored with a ^{233}Pa spike and a ^{234}Th spike, respectively. Recoveries were recorded by gamma spectrometry and were used to optimize the extraction and the separation of Pa and Th. In order to minimize geometry problems inherent to gamma spectrometry measurements, the same kind of Teflon[®] beakers, and the same amount of sample (*ca.* 1 mL) were used throughout each experiment. The duration (*ca.* 10 min) of each counting was the same for each experiment. The recovery was evaluated by normalizing the number of counts to the number of counts of the ^{233}Pa and ^{234}Th spikes just before they were added to the sample. The recovery for each fraction collected during the elution is indicated by bars in the following graphics.

6.2 - Anion exchange chromatography on AG1-X8 resin

The procedure is described in details in the previous paper. Only the results of tracer experiment are presented hereafter.

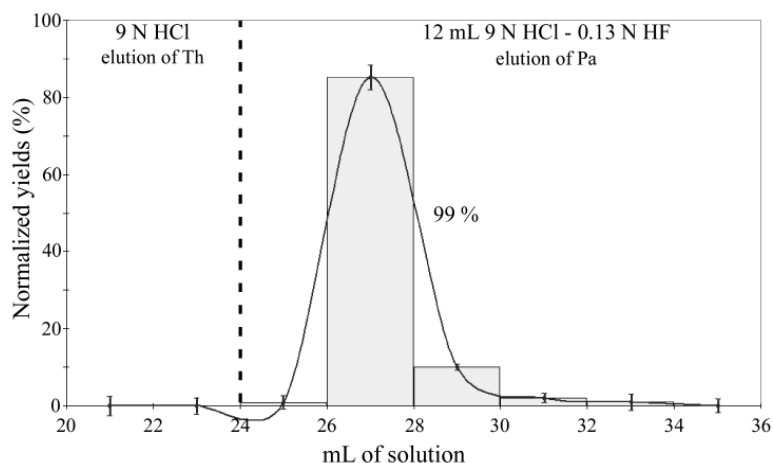


Figure 7 - Elution curve of Pa on the 4 mL AG1-X8 column used to separate Pa from Th and the major elements. The negative yield is an artefact linked to the graphic software. 2σ error bars are based on the analyses of 7 sediment samples.

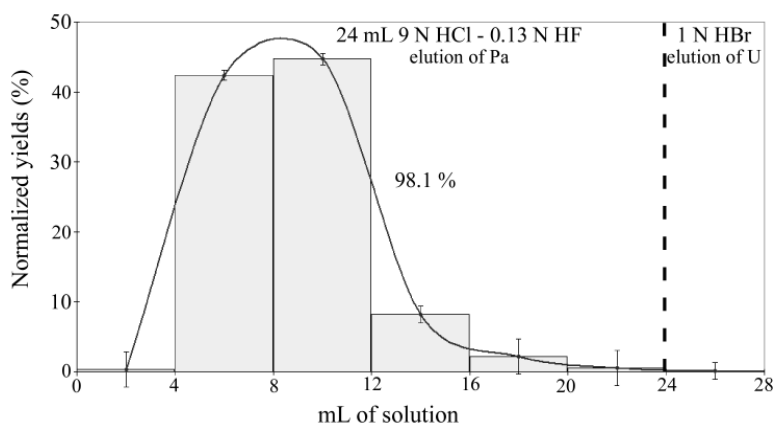


Figure 8 - Elution curve of Pa on the 4 mL AG1-X8 column used to purify the Pa fraction and maximize the separation between Pa and U. 2σ error bars are based on the analyses of 6 sediment samples.

Tracer experiments for AG1-X8 exchange chromatography were performed both at WHOI using a ^{233}Pa spike produced following the procedure of Anderson and Fleer (1982) and at the ENS Lyon using a ^{233}Pa spike produced following the procedure of Bourdon et al. (1999). Results are reported in figures 1 and 2. The overall yields are $98 \pm 8 \%$ for Pa. This elution procedure shows fairly reproducible yields. The main disadvantage comes from the time needed to run the entire chemical preparation and Pa-Th-U separation, i.e., about 10 days for 14 samples plus 2 blanks.

6.3 - Reverse phase chromatography with TRU-Spec[®] (Eichrom technologies, Inc)

The TRU SPEC[®] resin is constituted of a solution of 13 % CMPO (octyl(phenyl)-*N, N*-diisobutyl-carbamoylmethylphosphine oxide) and 27 % TBP (tributyl phosphate) adsorbed on an inert phase (e.g. Amberlite XAD-7) (Horwitz et al., 1990; 1993; Huff and Huff, 1993; Burnett and Yeh, 1995). The main extractant is CMPO, but it needs to be dissolved in TBP as it is solid at room temperature.

operation	solution	volume
preconditioning	H ₂ O	5 c.v.
	2 N HNO ₃	5 c.v.
sample loading	2 N HNO ₃	5 c.v.
elution of major elements	2 N HNO ₃	7.5 c.v.
conversion to chloride form	9 N HCl	1 c.v.
elution of R.E.E.	4 N HCl	10 c.v.
elution of Th	1 N HCl	7.5 c.v.
elution of U and Pa	0.1 N HCl - 0.1 N HF	10 c.v.

Table 9 - Th, Pa, and U elution procedure on a 2 mL TRU-Spec (50-100 μm) column. c.v. stands for column volume, i.e., 2 mL.

The method has been developed after the work of Burnett and Yeh (1995). The spiking and sample dissolution procedure used is the presented in the previous paper (Pichat et al., in preparation). The best results for the chromatographic separation are

obtained using a two-step procedure. The major elements, the rare Earth elements, and Th are separated from a fraction that contains U and Pa on a pre-packed 2 mL TRU-Spec (50-100 μm) column (table 1). This step is followed by the separation of U and Pa by anion exchange on a 1 mL AG1-X8 (200-400 mesh) column (table 2).

operation	acid	volume
preconditioning	H ₂ O	1 c.v.
	concentrated HCl - H ₂ O ₂	4 c.v.
sample loading	concentrated HCl - H ₂ O ₂	1 c.v.
column rinse	concentrated HCl - H ₂ O ₂	4 c.v.
	10 N HCl - H ₂ O ₂	2 c.v.
	8 N HCl - H ₂ O ₂	4 c.v.
	6 N HCl - H ₂ O ₂	3 c.v.
elution of Pa	8 N HCl - 0.05 N HF	5 c.v.
elution of U	H ₂ O	2 c.v.
	1 N HBr	2 c.v.

Table 10 - Pa and U separation on a 1 mL AG1-X8 (200-400 mesh) column. c.v. stands for column volume, i.e., 1 mL.

Results of these two elutions are presented in figures 3 and 4 for the TRU-Spec and AG1-X8 column, respectively. The overall yields are $94 \pm 5 \%$ for Pa and $96 \pm 5 \%$ for Th. The elution of Pa from the TRU-Spec column is made with 0.1 N HCl - 0.1 N HF which also entrains TBP because of its solubility in water and low concentrated acids. Part of this organic acid is removed via the use of the AG1-X8 column; however, the removal of TBP is not efficient enough. It decreases the Pa recovery to $50 \pm 10 \%$ in the 0.8 N HNO₃ - 0.05 N HF solution used to inject the sample in the ICP-MS. For the Th the recovery is decreased to $75 \pm 10 \%$ in the 0.8 N HNO₃ solution used to inject the sample in the ICP-MS. With the procedure described in section 6.2 the recovery for both isotopes for this step is close to 100 %. Because of this problem, we have chosen to use the method described in section 6.2.

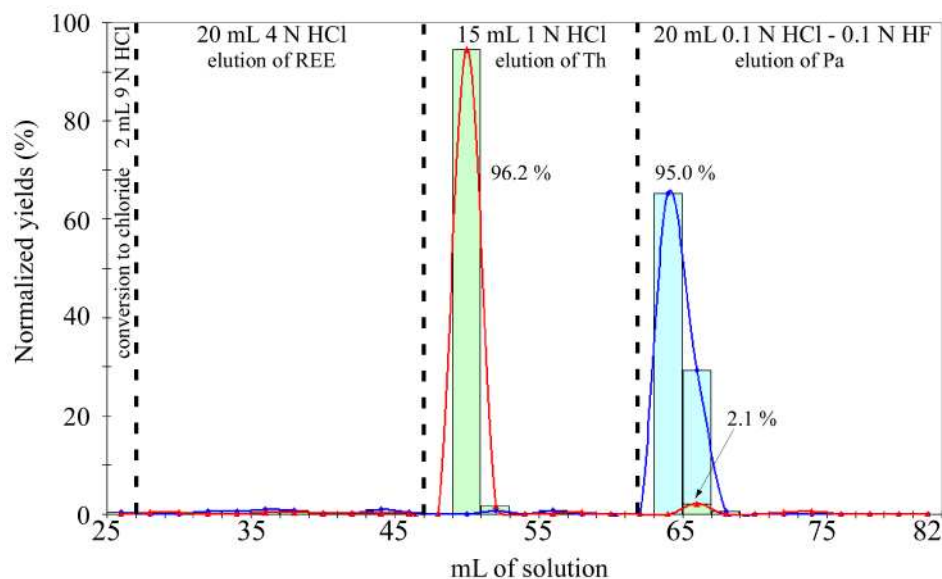


Figure 9 - Elution curves of Th and Pa on a 2 mL TRU-Spec column used to separate U, Th, and Pa from the matrix, following the procedure described in table 1. The elution curves for Th and Pa are represented in red and blue, respectively. The bars indicate the amount of Th (green) and Pa (blue) presents in each fraction collected.

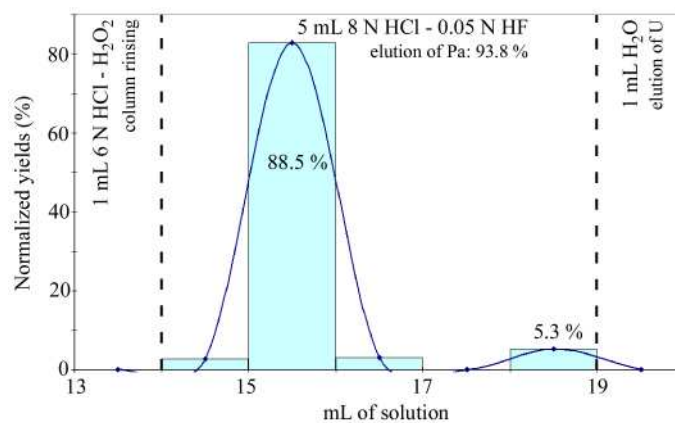


Figure 10 - Elution curve of Pa on a 1 mL AG1-X8 column used to purify the Pa fraction and maximize the separation between Pa and U, following the procedure described in table 2. The elution curve for Pa is represented in blue and the recovery for each fraction collected during the elution is indicated by a blue bar.

6.4 - Reverse phase chromatography with HDEHP

We have used di-(2-ethylhexyl) phosphoric acid (HDEHP) (e.g. Ghersini, 1975) coated on polytrifluorochloroethylene (PFCE) ($-\text{[CF}_2\text{CFCl]}_n-$) balls (Votalef 300 CHR, 300 LD, micro PL, ELF) to extract Pa and Th from the matrix. Then, Pa and Th were separated by anion exchange chromatography. After its elution from the HDEHP column, U was also separated from the matrix by anion exchange chromatography.

0.25 g of sediment was used. The dissolution method, summarized in table 3, did not involve a precipitation of iron oxihydroxides. The sample was then loaded on a 2.5 mL HDEHP column made of Teflon[®] (6.4 mm internal diameter, 7.5 cm long, and surmounted by a 15 mL reservoir). The elution method is summarized in table 4. Figure 5 shows the elution curve for Pa.

Elimination of carbonates	1-2 mL of 9 N HCl
Spiking	^{233}Pa , ^{236}U , ^{229}Th
Overnight equilibration	
Dissolution and elimination of organic matter	5 mL of conc. HF, 3-4 mL of conc. HClO_4 , 3 mL of 9 N HCl
Evaporation to near dryness at 200° C, elimination of fluorides ions	
Preparation for load on HDEHP column	2 mL of 9 N HCl

Table 11 - Summary of the dissolution of deep-sea sediments prior to Th-Pa-U separation by reverse phase chromatography on a HDEHP column. Conc. stands for concentrated.

Load	2 mL of 9 N HCl
Elution of major elements, lanthanides ⁽¹⁾ and U	8 mL of 9 N HCl
	3 mL of 2.5 N HCl
Elution of Pa and Th	7 mL of 9 N HCl - 0.13 N HF

Table 12 - Summary of the separation of Th, Pa and U on a 2.5 mL HDEHP column.

⁽¹⁾ Qureshi et al., 1969.

U was separated from the matrix by anion exchange chromatography (AG1-X8 resin) using a classical procedure (Goldstein et al., 1989; Goldstein et al., 1991). 1-2 mL of concentrated HClO_4 was added to the Pa-Th fraction which was then evaporated to near dryness at 200°C in order to remove the fluoride ions. The sample was then dissolved in 1 mL of 9 N HCl and loaded on a 1 mL AG1-X8 column to separate Pa from Th. The elution procedure is summarized in table 5, and the elution curve for Pa is shown in figure 6.

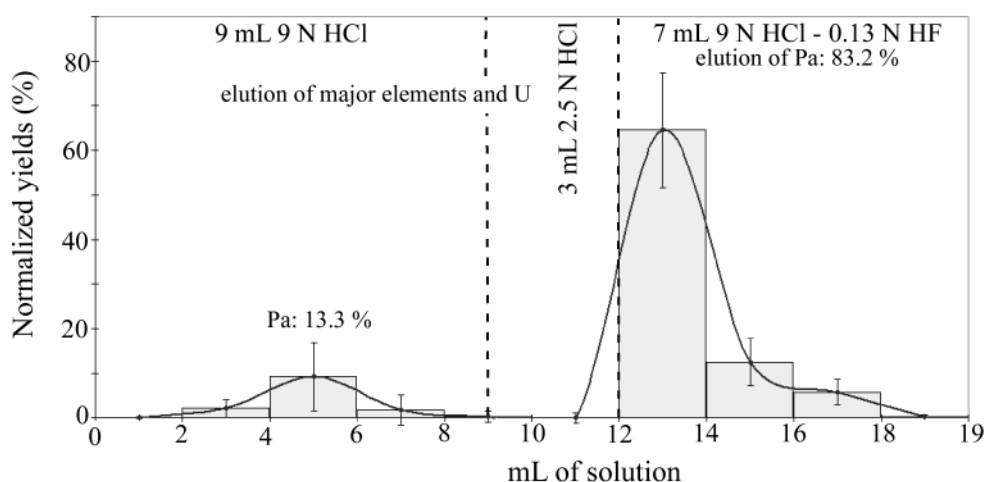


Figure 11 - Elution curve for Pa on a 2.5 ml HDEHP column following the elution procedure described in table 4. 2σ error bars are based on the analyses of 12 sediment samples (cf. table 6).

Load	2 mL of 9 N HCl
Elution of Th	8 mL of 9 N HCl
Elution of Pa	5 mL of 9 N HCl - 0.13 N HF

Table 13 - Summary of the separation of Pa and Th on a 1 mL AG1-X8 column.

The procedure described above has been tested by ICP-MS for U and Th but not for Pa. U and Th showed overall procedural yields higher than 90 %. However, this procedure presents a major disadvantage for Pa since fluorides complexes (PaF_7^{2-}) are not always totally removed by the perchloric acid fuming step. Consequently, the overall procedural Pa recovery is highly variable. Approximately 20 % of the samples showed an overall Pa recovery lower than 25 %, presumably because of the presence of fluorides

complexes that prevents the adsorption of Pa on HDEHP and AG1-X8. These led us to reject the method and prefer the one described in section 6.2. An example of overall Pa recovery for fourteen samples is presented in table 6.

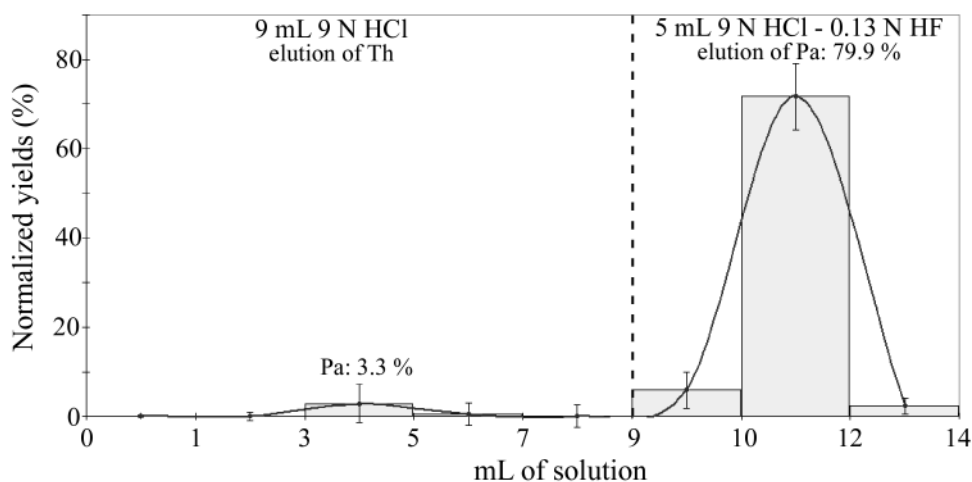


Figure 12 - Elution curve for Pa on a 1 ml AG1-X8 column following the elution procedure described in table 5. 2σ error bars are based on the analyses of 12 sediment samples (cf. table 7).

sample	Pa overall recovery (%)	sample	Pa overall recovery (%)
SU 0-1,5	84.9	SU 160-162	58.2
SU 20-24	78.4	SU 180-184	96.3
SU 40-42	80.7	SU 200-202	66.1
SU 60-62	62.1	SU 220-222	87.1
SU 80-84	90.4	SU 240-242	95.5
SU 100-102	86.5	SU 260-262	73.2
SU 140-142 ⁽¹⁾	0.7	SU 280-282 ⁽¹⁾	5.9
	average (%)		79.9
	std dev. (%)		12.7
	2 s err. (%)		9.1

Table 14 - Overall Pa recovery for 14 Atlantic deep-sea sediment samples using HDEHP reverse phase chromatography followed by anion exchange chromatography. ⁽¹⁾These samples have not been taken into account for the overall recovery statistic calculations.

Bibliographie

- Anderson, R. F., and A. P. Fleer, Determination of natural actinides and plutonium in marine particulate material, *Anal. Chem.* **54**, 1142-1147, 1982.
- Archer, D. E., Equatorial Pacific calcite preservation cycles: production or dissolution ?, *Paleoceanography* **6**, 561-571, 1991.
- Bourdon, B., J.-L. Joron, and C. J. Allègre, A method for ^{231}Pa analysis by thermal ionization mass spectrometry in silicate rocks, *Chem. Geol.* **157**, 147-151, 1999.
- Burnett, W. and C. C. Yeh, Separation of Protactinium from Geochemical Materials via Extraction Chromatography, *Radioact. Radiochem.* **6**, 22-26, 1995.
- Choi, M. S., R. François, K. Sims, M. P. Bacon, S. Brown-Leger, A. P. Fleer, L. A. Ball, D. Schneider, and S. Pichat, Rapid determination of ^{230}Th and ^{231}Pa in seawater by desolvated micro-nebulization inductively coupled plasma magnetic sector mass spectrometry, submitted to *Rapid Com. Mass Spectrom.*
- Fleer, A.P., and M. P. Bacon, Notes on some techniques of marine particle analysis used at WHOI. In *Marine Particles: Analysis and Characterization*, Hurd, D. C., and D. W. Spencer (Eds), *Geophys. Monograph.* **63**, AGU, 223-226, 1991.
- Ghersini, G., Stationary phases in extraction chromatography. In *Extraction chromatography*, Braun, T., G. Ghersini (Eds), J. Chrom. Library, Vol. 2, Elsevier, Amsterdam, The Netherlands, 68-133, 1975.
- Goldstein, S. J., M. T. Murrell, D. R. Janecky, J. R. Delaney, and D. A. Clague, Geochronology and petrogenesis of MORB from the Juan de Fuca and Gorda ridges by U-Th disequilibrium, *Earth Planet. Sci. Lett.* **104**, 513-534, 1991.
- Goldstein, S. J., M. T. Murrell, and D. R. Janecky, Th and U isotopic systematics of basalts from the Juan de Fuca and Gorda Ridges by mass spectrometry, *Earth Planet. Sci. Lett.* **96**, 134-146, 1989.

- Horwitz, E. P., R. Chiarizia, M. L. Dietz, H. Diamond, and D. M. Nelson, Separation and preconcentration of actinides from acidic media by extraction chromatography. *Anal. Chim. Acta* **281**, 361–372, 1993.
- Horwitz, E. P., M. L. Dietz, D. M. Nelson, J. J. LaRosa, and W. D. Fairman, Concentration and separation of actinides from urine using a supported bifunctional organophosphorus extractant, *Anal. Chim. Acta* **238**, 263–271, 1990.
- Huff, E. A., and D. R. Huff, TRU-Spec and RE-Spec chromatography: Basic studies and applications. *34th ORNL/DOE Conf. on Anal. Chem. in Energy Technology*, Gatlinburg, TN, 1993.
- Isern, A. R., Calcium carbonate and organic carbon accumulation in the Central Equatorial Pacific, M.S. thesis, Grad. Sch. Oceanogr., Univ. R.I., Narragansett, RI, U.S.A., 197 pp, 1991.
- Lyle, M., D. W. Murray, B. P. Finney, J. Dymond, J. M. Robbins, and K. Brooksforce, The record of the late Pleistocene biogenic sedimentation of the eastern tropical Pacific Ocean, *Paleoceanography* **3**, 39-59, 1988.
- Marcantonio F., R. F. Anderson, S. Higgins, M. Stute, and P. Schloesser, Sediment focusing in the central equatorial Pacific Ocean, *Paleoceanography* **16**, 260-267, 2001.
- Paytan, A., M. Kastner, and F. Chavez, Glacial to interglacial fluctuations in productivity in the equatorial Pacific as indicated by marine barite, *Science* **274**, 1355-1357, 1996.
- Pichat, S., K. W. Sims, R. François, J. F. McManus, and F. Albarède, Lower biological productivity during glacial periods in the equatorial Pacific as derived from $(^{231}\text{Pa}/^{230}\text{Th})_{\text{xs},0}$ measurements in deep-sea sediments, in preparation.
- Pichat, S., Etudes préliminaires à la mesure du rapport $^{231}\text{Pa}/^{230}\text{Th}$ par ICP-MS dans des sédiments carbonatés marins: mise au point d'une méthode d'extraction et de séparation chromatographique, *mémoire de D.E.A.*, Université Grenoble I, 50 pp., 1997.
- Qureshi I. H., L. T. McClendon, and P. D. Lafleur, Extraction studies of the group IIIB-VIIB elements and the lanthanides utilizing bis(2-ethyl-hexyl)orthophosphoric acid, *Radiochim. Acta* **12**, 107-111, 1969.

Sigman, D. M., and E. A. Boyle, Glacial/interglacial variations in the atmospheric carbon dioxide, *Nature* **407**, 859-869, 2000.

Wefer, G., W. H. Berger, J. Bijma, and G. Fischer, Clue to ocean history: a brief overview of proxies. In *Use of proxies in paleoceanography: Examples from the South Atlantic*, Fischer, G., and G. Wefer (Eds), Springer-Verlag, Berlin Heidelberg, Germany, 1-68, 1999.